

(12)

RF Project 762134/712823
Topical Report

AD A119350

**the
ohio
state
university**

research foundation

1314 kinnear road
columbus, ohio
43212

PACKING OF OXIDE CERAMIC POWDERS
BY CENTRIFUGAL CASTING

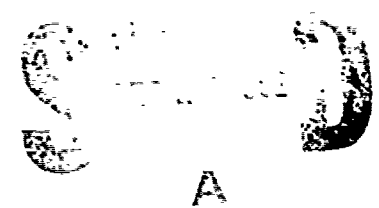
G. W. Shaffer and D. W. Readey
Department of Ceramic Engineering

DEPARTMENT OF THE NAVY
Office of Naval Research
Arlington, Virginia 22217

Contract No. N00014-80-C-0523

DTIC FILE COPY

September, 1982



82 09 20 005

This document has been approved
for public release and sale; its
distribution is unlimited.

Unclassified

SECURITY CLASSIFICATION OF THIS PAGE (When Data Entered)

REPORT DOCUMENTATION PAGE		READ INSTRUCTIONS BEFORE COMPLETING FORM
1. REPORT NUMBER	2. GOVT ACCESSION NO. PB-PH9350	3. RECIPIENT'S CATALOG NUMBER
4. TITLE (and Subtitle) PACKING OF OXIDE CERAMIC POWDERS BY CENTRIFUGAL CASTING		5. TYPE OF REPORT & PERIOD COVERED Topical Report
		6. PERFORMING ORG. REPORT NUMBER 762134/712823
7. AUTHOR(s) G.W. Shaffer and D. W. Readey		8. CONTRACT OR GRANT NUMBER(s) Contract No. N00014-80-C-0523
		10. PROGRAM ELEMENT, PROJECT, TASK AREA & WORK UNIT NUMBERS NR 032-602/3-2480 471
9. PERFORMING ORGANIZATION NAME AND ADDRESS The Ohio State University Research Foundation, 1314 Kinnear Road Columbus, Ohio 43212		12. REPORT DATE September, 1982
11. CONTROLLING OFFICE NAME AND ADDRESS DEPARTMENT OF THE NAVY Office of Naval Research Arlington, Virginia 22217		13. NUMBER OF PAGES 99
		15. SECURITY CLASS. (of this report) Unclassified
14. MONITORING AGENCY NAME & ADDRESS (if different from Controlling Office)		15a. DECLASSIFICATION/DOWNGRADING SCHEDULE
16. DISTRIBUTION STATEMENT (of this Report) Approved for public release; distribution unlimited.		
17. DISTRIBUTION STATEMENT (of the abstract entered in Block 20, if different from Report)		
18. SUPPLEMENTARY NOTES		
19. KEY WORDS (Continue on reverse side if necessary and identify by block number) ceramic powders oxides casting centrifugal casting		
20. ABSTRACT (Continue on reverse side if necessary and identify by block number) Topical commercially available powders of silica, zinc oxide, tin oxide, and alumina were centrifugally cast. The purpose of the study was to determine the feasibility of centrifugal casting well-dispersed slips of such ceramic oxide powders to obtain high green densities and to observe the effects that deviations from an ideal monodisperse, spherical powder have on the resulting packing density. The powders were characterized by particle size		

DD FORM 1 JAN 73 1473

EDITION OF 1 NOV 55 IS OBSOLETE

Unclassified

SECURITY CLASSIFICATION OF THIS PAGE (When Data Entered)

Block 20--Abstract (Continued)

distributions and microscopy. Viscosity versus pH data were obtained for those powders for which there was a sufficient quantity. The results generally showed a good correlation of centrifugal casting density with the degree of powder dispersion as measured by viscosity. However, the packing densities obtained were not higher than those which can be obtained by conventional slip casting or dry pressing. It can be concluded that centrifugal casting of typical ceramic powders does not offer any advantage over other consolidation processes.

PACKING OF OXIDE CERAMIC POWDERS
BY CENTRIFUGAL CASTING

G. W. Shaffer and D. W. Readey
Department of Ceramic Engineering
The Ohio State University

September 1982



A

TABLE OF CONTENTS

	<u>Page</u>
I. INTRODUCTION	11
II. THEORY	15
A. Van der Waals Forces	15
B. Repulsive Forces	17
C. Approach to Ideal Packing	18
D. Centrifugal Casting	20
III. EXPERIMENTAL PROCEDURE	21
A. Powders	21
B. Slip Preparation	22
C. Centrifugal Casting	25
IV. RESULTS	29
A. SiO ₂	29
1. Powder Characterization	29
a. General	29
b. Spherisorb Powder	36
c. Fume	38
2. Casting	38
a. General	38
b. Spherisorb Powder	38
c. Fume	47
B. ZnO	48
1. Powder Characterization	48
2. Viscosity Versus pH	55
3. Casting	57
a. As-received Powder	57
b. Fines Only	60
c. Ball-milled Powder	62

TABLE OF CONTENTS (CONTD.)

	<u>Page</u>
C. SnO ₂	65
1. Powder Characterization	65
2. Viscosity Versus pH	65
3. Casting	65
D. Al ₂ O ₃	73
1. Powder Characterization	73
2. Viscosity Versus pH	79
3. Casting	80
V. DISCUSSION	87
A. SiO ₂	87
B. ZnO	89
C. SnO ₂	91
D. Al ₂ O ₃	91
VI. CONCLUSIONS	93
VII. REFERENCES	95

LIST OF ILLUSTRATIONS

<u>Figure</u>	<u>Title</u>	<u>Page</u>
1	The effect of the particle separation distance on the total potential energy of interaction	19
2	The particle size distribution of the 5 μ Min-u-Sil SiO ₂	30
3	The particle size distribution of the 5 μ Spherisorb SiO ₂	31
4	The particle size distribution of the 10 μ Spherisorb SiO ₂	32
5	The particle size distribution of the SiO ₂ fume. (Curve 1 is the particle size distribution curve, and Curve 2 is a Gaussian best fit distribution of Curve 1	33
6	SEM Micrograph of the 5 μ Min-u-Sil SiO ₂ . 7000X	34
7	SEM Micrograph of the 5 μ Spherisorb SiO ₂ . 2000X	34
8	SEM Micrograph of the 10 μ Spherisorb SiO ₂ . 1000X	35
9	TEM Micrograph of the SiO ₂ . 76,800X	35
10	X-ray diffraction pattern of 5 μ Spherisorb SiO ₂	37
11	The effect of pH on the centrifugal packing density for the 5 μ Spherisorb SiO ₂	40
12	The effect of the concentration of powder in the slip on the centrifugal packing density of the 5 μ Spherisorb SiO ₂	44

LIST OF ILLUSTRATIONS (CONT.)

<u>Figure</u>	<u>Title</u>	<u>Page</u>
13	The effect of the viscosity of the settling medium on the packing density of the 5 μ Spherisorb SiO ₂	45
14	SEM Micrograph of the packing of the 5 μ Spherisorb SiO ₂ . 368X	46
15	SEM Micrograph of a centrifugally cast packing of the 5 μ Spherisorb SiO ₂ . 700X	46
16	SEM Micrograph of a centrifugally cast packing of the SiO ₂ fume. 48,000X	49
17	The particle size distribution of the Baker Reagent ZnO	50
18	The particle size distribution of the St. Joe's #17 ZnO	51
19	The particle size distribution of the St. Joe's #30 ZnO	52
20	The particle size distribution of the St. Joe's #100 ZnO	53
21	SEM Micrograph of the Baker Reagent ZnO. 7000X	54
22	SEM Micrograph of the St. Joe's #100 ZnO. 23,200X	54
23	The effect of pH on the viscosity of the slip for the St. Joe's #100 ZnO - Trial 2	56
24	The effect of the concentration of powder in the slip on the centrifugal packing density of the St. Joe's #100 ZnO	59
25	The particle size distribution of the St. Joe's #100 ZnO that was dry ball milled 6 $\frac{1}{2}$ hours and then wet ball milled for 5 $\frac{1}{2}$ more hours	63

LIST OF ILLUSTRATIONS (CONT.)

<u>Figure</u>	<u>Title</u>	<u>Page</u>
26	TEM Micrograph of the ball milled St. Joe's #100 ZnO. 12,800X	64
27	The particle size distribution of the SnO ₂	66
28	TEM Micrograph of the SnO ₂ . 12,800X	67
29	The effect of pH on the viscosity of the slip for the SnO ₂	68
30	The effect of pH on the centrifugal packing density for the SnO ₂	69
31	The particle size distribution of the SnO ₂ after the larger particles were removed by settling	71
32	The effect of the concentration of powder in the slip on the centrifugal packing density of the SnO ₂	72
33	The particle size distribution of the .1µm polishing Al ₂ O ₃	74
34	The particle size distribution of the Alcoa A-17 Al ₂ O ₃	75
35	The particle size distribution of the Reynolds RC-152 Al ₂ O ₃	76
36	SEM Micrograph of the .1µ polishing Al ₂ O ₃ from Fisher Scientific Co. 700X	77
37	SEM Micrograph of the Alcoa A-17 Al ₂ O ₃ . 3000X	77
38	SEM Micrograph of the Reynolds RC-152 Al ₂ O ₃ . 5000X	78
39	The effect of pH on the viscosity of a 73% solids by volume slip of the Alcoa A-17 Al ₂ O ₃	81
40	The effect of pH on the viscosity of a 20% solids by volume slip of the Alcoa A-17 Al ₂ O ₃	82

LIST OF ILLUSTRATIONS (CONT.)

<u>Figure</u>	<u>Title</u>	<u>Page</u>
41	The effect of pH on the centrifugal packing density for the Alcoa A-17 Al ₂ O ₃	83
42	The effect of the concentration of powder in the slip on the centrifugal packing density of the Alcoa A-17 Al ₂ O ₃	86

LIST OF TABLES

<u>Table</u>	<u>Title</u>	<u>Page</u>
1	Centrifugal Packing Density as a Function of Dispersant for 5μ SiO_2	42
2	pH vs Centrifugal Packing Density for St. Joe's #100 ZnO - Trials 1 and 2	58
3	pH vs Centrifugal Packing Density for St. Joe's #100 ZnO , (Particle Size $<1\mu$)	61
4	Centrifugal Packing Density as a Function Function of Dispersant for St. Joe's #100 #100 ZnO (Particle Size $<1\mu$)	61
5	Centrifugally Cast Packing Densities of 37% solids by Volume Alcoa A-17 Al_2O_3 Slip at pH 2 and 11	84
6	Packing Density of Slip Cast Alcoa A-17 Al_2O_3 , (pH of Slip was 2)	84

PACKING OF OXIDE CERAMIC POWDERS
BY CENTRIFUGAL CASTING

I. INTRODUCTION

The initial packing of powders plays an extremely important role in subsequent microstructure development and probably is the most neglected area of powder processing both during the technological preparation of materials and the investigation of fundamental mechanisms. For example, the stages in solid state sintering for the purpose of analysis and description have been broken down into: 1. initial (neck growth between particles); 2. intermediate (continuous pore channels); and 3. final (isolated pores)¹. All of these assume that a uniform pore-particle geometry exists throughout a powder compact so that the overall shrinkage of a compact (the frequently used measure of densification or microstructure development) can be modeled from the average pore-particle geometry of essentially close-packed particles. If proper care is taken, certainly close-packing of particles in the intermediate and final stages of densification is close to the actual situation existing in a real compact. On the other hand, in real powder compacts, particularly those made by powder pressing, the initial particle packing is

usually far from ideal close-packed. Face-centered-cubic packing of uniform spheres gives a packing density of 74 percent of theoretical² and packing of particles of mixed sizes³ or even particles with a continuous particle size distribution⁴ can lead to even higher packing densities. Yet it is experimentally observed both macroscopically^{5,6} and microscopically⁷ that packing densities are frequently lower than this, typically between 50 and 60 percent of theoretical. The theoretical density of particles packed in a simple cubic array is 52 percent and an as-pressed powder is more typical of a simple cubic array with an average number of around six nearest neighbors per particle. Therefore, during the initial stage of densification, a significant geometric rearrangement must occur in which the average number of particle contacts changes from six to around twelve, going from an open to a close-packed structure with attendant 20-25 percent volume change!⁸

This rapidly changing geometry during the initial stage of sintering makes the application of either shrinkage⁹ or surface area changes^{10,11} to powder compacts of small particle size a somewhat dubious method for the determination of sintering kinetics and mechanisms.

Therefore, the attainment of ideal close-packed particle packing is highly desirable for confirmation of initial stage sintering models and more importantly, to observe the

effects of deviations from ideality such as impurities, second phases or neck growth without shrinkage. Furthermore, with an ideally packed material, the transition from the initial, to intermediate to final stages of densification can be more easily modeled and followed. Of primary importance, since ideal compacts are probably not likely for "real" ceramic materials of interest, deviations from an ideal compact both in packing arrangement and deviation of the particles from spheres or from a monodisperse particle size distribution and their effect on sintering can be observed.

II. THEORY

A. Van der Waals Forces

Large spheres can be vibrated to produce ideal close-packed arrays³ but the van der Waals-London attractive force between small powder particles less than about one micrometer in size produces agglomerates and non-ideal powder packing typically about 50-60 percent of theoretical density.¹² Van der Waals forces are generally considered to be weak forces which rapidly fall off with interparticle separation since the force between two atoms is inversely proportional to their separation to the sixth power. That is,¹³

$$f_{\text{attractive}} = - \frac{\lambda}{r^6}$$

where λ = constant and r = separation distance.

For macroscopic bodies, this force has to be integrated between all atom pairs with the result for two spheres of radius a at a separation distance r ¹⁴, for $r \ll a$;

$$f = \frac{Aa^2}{12r^2}$$

where $A = \pi^2 n^2 \lambda \approx 10^{-12}$ erg.

n = atomic density in the solid

Therefore, van der Waals forces between macroscopic bodies are proportional to the size of the body and only fall off as the inverse square of the particle separation.¹⁴ To obtain "free-flowing" particles, the type which is desirable for die-filling during dry pressing of powders, the gravitational force causing the particles to roll freely past one another should be large compared to van der Waals forces.

For the particle sizes used for the preparation of ceramic materials ($a \leq 1\mu\text{m}$) van der Waals forces dominate the flow behavior and prevent close packing by forming bridges. As a result, die pressing rarely results in packing densities much in excess of 60 percent of theoretical regardless of the pressure. High pressures (50,000 psi) lead to higher packing densities by plastic deformation or fracturing of the particles.¹⁵ If the particles are agglomerates, high pressure causes compaction or fracturing of the agglomerates^{16,17} and compaction versus pressure can be used as a measure of the strength of the agglomerates

and the degree of powder agglomeration.¹⁶ Nevertheless, high pressure compaction rarely leads to green densities in excess of 70 percent of theoretical in spite of the fact that with the smaller fractured particles, densities above 80 percent are possible.³ Such non-ideal and non-uniform packing is not conducive to pore-free microstructure development nor is it a good starting point for the study of the mechanism and factors influencing microstructure development.

B. Repulsive Forces

A much more sanguine environment conducive to the development of ideal particle packing is found in a suspension of the powder in an electrolyte solution. In an electrolyte, the surfaces of solid particles acquire an adsorbed charge of "potential-determining" ions. Surroundings each particle there is a higher concentration of oppositely-charged "counter ions" which neutralize the adsorbed surface charge. This charged "double layer" leads to an electrostatic potential^{14,18} and a repulsive force between particles. Therefore, in an electrolyte, powder particles can be kept from agglomerating up to solid contents in excess of 70 percent by volume. This, of course, is the basis of slip casting and high specific gravity slips can produce castings with densities in excess of 80 percent

of theoretical.¹⁹ Coagulation of the dispersed powder will occur when the repulsive electrostatic forces just balance the attractive van der Waals forces as shown in Figure 1. Therefore, the specific gravity of a casting slip and the resulting cast density can be controlled by the concentration and valence of the ions in solution which control the double layer thickness. An optimum casting slip is one in which the electrolyte concentration is adjusted so that the repulsive forces just exceed the attractive forces to give the smallest separation distance between particles (to obtain the highest specific gravity) yet maintain a stable slip²⁰.

C. Approach to Ideal Packing

Densities above 80 percent of theoretical are possible in slip cast pieces because the typical slip is made by milling which produces a wide particle size distribution leading to more efficient particle packing than can be obtained with monodisperse material. However, with the balancing of the attractive van der Waals forces against the repulsive electrostatic forces in an electrolyte, ideal packing of monodisperse particles may be approached. Green densities in excess of 70 percent of theoretical have been obtained with centrifugally cast suspensions from which agglomerates had been removed.^{21,22} These very fine zirconia particles, thought to be individual

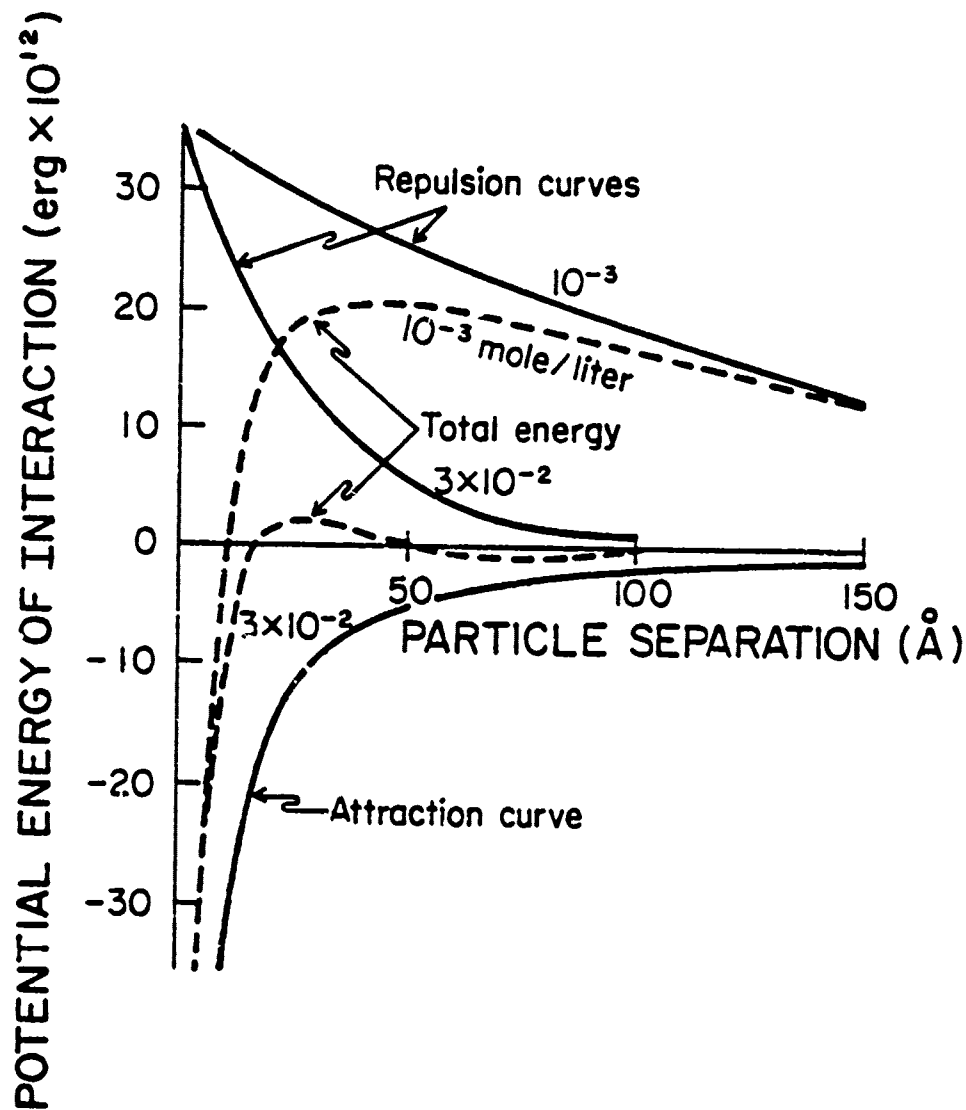


Figure 1. The effect of the particle separation distance on the total potential energy of interaction.⁹

crystallites, sintered to almost theoretical density at a relatively low temperature with a final grain size of only 0.2 micrometers. This important result demonstrates:

- 1) the importance of removing agglomerates;
- 2) the possibility of achieving almost ideal packing of small almost monodisperse particles;
- 3) the possibility of obtaining complete densification with an ideally packed monodisperse array of particles; and most importantly
- 4) obtaining high green density by centrifugal casting.

Latex spheres have been used to demonstrate close packing of charged particles in the laboratory.^{23,24,25} Opals consist of close-packed arrays of silica particles precipitated and settled from solution.^{26,27,28}

D. Centrifugal Casting

There is adequate theoretical and experimental evidence to conclude that high density, close-packed particle arrays can be obtained from carefully controlled electrolyte suspensions. Therefore, part of this research was to evaluate centrifugal casting as a means of forming ideal powder particulate compacts by settling from dispersed aqueous suspensions mono-sized spherical powder particles. In parallel with this effort, the centrifugal casting of some more typical ceramic powders was evaluated to determine the effects that deviations from ideality had; and, equally important, to evaluate centrifugal casting as a consolidation process for "real" powders.

III. EXPERIMENTAL PROCEDURE

A. Powders

In order to perform the centrifugal packing studies in parallel with the powder preparation, several commercial powders were investigated. The first step consisted of determining suitable oxide powders on which to conduct the experiments. A particle size analysis was performed to ensure that the powders had a small size and a narrow distribution in the 1-10 μm range or smaller. This was accomplished with a sedimentation apparatus^{*} or by semi-automatic image analysis of electron micrographs.^{**} The latter technique permitted the evaluation of particle shape, with the goal of finding nonagglomerated, spherical particles. Other tests on powders, when necessary, included measuring the specific gravity (Standard ASTM pycnometer test, C-135), x-ray analysis to determine if they were amorphous or crystalline, differential thermal analysis to determine if any adsorbed or chemical water were present, and finally, making sure the acid and base dispersants had

* MSA Particle Size Analyzer

** Zeiss Videoplan

no detrimental effects. The powders chosen in this project were SiO_2 , ZnO , SnO_2 , and Al_2O_3 . Detailed descriptions of these powders are given later.

B. Slip Preparation

In most cases, a viscosity versus pH test was done for each oxide to find the pH at maximum dispersion; i.e., minimum viscosity. A slip was prepared by mixing the powder and water with a Waring blender. A flowable slip, with as high a solids content as possible, was used. The viscosity was measured with a Brookfield viscometer and an average of six readings was used for the viscosity versus pH curve. The pH of the slip was measured both before and after the viscosity determination to ensure that it had not changed. The acids and base used for dispersion were HCl , HNO_3 , HF , and NH_4OH .* In addition, other dispersants were used in some of the experiments.

A list of these dispersants and a description, if necessary, of each is as follows:

1. Acetone
2. Darvan #7 - This is an organic polyelectrolyte manufactured by the R. T. Vanderbilt Co., Inc. (230 Park Ave., New York NY).

*Fisher Reagent Grade.

3. "Feeding Solution" - For 1000 ml of solution this consists of 700 ml of distilled H₂O, 300 ml of acetone and 90 drops of Darvan #7.
4. Sodium Silicate.
5. Potassium Silicate.
6. Tri-sodium Phosphate.
7. Mighty 150 - this is a wetting agent used in the cement industry. It is a strong SiO₂ dispersant. This product is a condensate of naphthalene formaldehyde. This product is manufactured by ICI America, (Wilmington, DE).
8. Melment L10 - This is also a strong SiO₂ dispersant used in the cement industry. It is a sulfonated melamine formaldehyde. This product is manufactured by the American Admixture Corp., (Chicago IL).

Experiments were performed to determine any correlation between centrifugal packing density and the powder concentration in the slip. The concentration of powder ranged from .036 to .214 gms/ml of solution in increments of .036 gms/ml of solution.

Lowering and narrowing the particle size distribution of a powder was done by a settling technique. About 20 grams of the powder were dispersed in 1000 ml of the feeding solution by a Waring blender. The solution was then poured into a 1000 ml graduated cylinder and allowed

to settle, undisturbed. The larger particles settled leaving the smaller ones in suspension. Knowing the particle size needed, the settling time was calculated from Stoke's Law. For example:

All particles 1 μ and above needed to be settled from a ZnO powder.

$$v = 2gr^2(d_1 - d_2)/9\eta$$

$$v = \frac{2(980 \text{ cm/sec}^2)(.5 \times 10^{-4} \text{ cm})^2(1.0 \text{ g/cm}^3 - 5.61 \text{ g/cm}^3)}{9(01 \text{ poise})}$$

$$v = 2.51 \times 10^{-4} \text{ cm/sec}$$

$$h = 34.5 \text{ cm (settling distance)}$$

$$\therefore t = 1.37 \times 10^5 \text{ sec} \sim 38.2 \text{ hours.}$$

It would take about 38.2 hours to settle all particles 1 μ and above. Also, knowing the particle size distribution of the ZnO, the amount of powder that would be retained in suspension was predicted. After the large particles had settled, the liquid was decanted and centrifuged to recover the smaller particles. After the powder was dry, it was used for centrifugal packing density studies, and these results were compared with the packing densities obtained with the larger particles.

C. Centrifugal Casting

For centrifugal casting experiments, the oxide powder was weighed, the amount depending on the density of the powder. A 1 to 2 ml packing volume was desired, so accurate readings of the packing volume could be read from a graduated centrifuge tube. Usually 1-2 grams of the powder were sufficient. Fourteen ml of each of solutions with the desired pH were placed in labeled, graduated centrifuge tubes, and the tubes placed in an ultrasonic bath. The powder was then slowly added to produce the slip. Then, the tubes were centrifuged in a Beckman J2-21 centrifuge. The time of centrifuging was determined by Stoke's Law, taking into account the centrifugal force.

That is:

$$v = 2gxr^2(d_1-d_2)/9\eta$$

where,

v = the velocity in cm/sec.

g = 980 cm/sec²

x = a factor to account for the centrifugal force.

This factor is dependent on the rotational speed of the centrifuge and the type of rotor being used.

$x = 1.12a$ (rpm/1000)² where, a = the radius of the rotor in millimeters.

r = the radius of the particles in cm.

d_1 = the density of the medium in gm/cm³

d_2 = the density of the particle in gm/cm³

η = the viscosity in Poise

From this equation the velocity was found since x , d_1 , d_2 , and η were known. The value for r was also known, from the particle size analysis. The height of the centrifuge tubes were known, therefore, the time of centrifuging was found from the following relation:

$$v = h/t$$

where,

v = the velocity in cm/sec.

h = the height of the centrifuge tube in cm.

t = the time for a particle to fall a height of h , in sec.

After centrifuging, the test tubes were removed, and the packing volumes were recorded from the height of the settled powder in centrifuge tube. Knowing the packing volumes and weight of powder, the percent theoretical densities were calculated from the following relation:

$$\% \text{ Theoretical Density} = \frac{W}{V} \cdot \rho_t \times 100$$

where,

W = the weight of the powder in the test tubes in grams.

V = the packing volume in cm^3 .

ρ_t = the theoretical density of the powder.

Usually, the powder could be redispersed in each test tube, and the experiment repeated. A pH versus packing density curve was then plotted.

IV. RESULTS

A. SiO₂

1. Powder Characterization

a. General. Four SiO₂ powders were under consideration for centrifugal slip casting studies. These were a 5 μ Min-u-sil SiO₂^{*}, a 5 μ and 10 μ Spherisorb SiO₂^{**} and a SiO₂ fume, (a by-product from the manufacture of silicon).^{***}

The particle size distributions for these powders are shown in Figures 2, 3, 4, and 5, respectively. Each powder has a relatively narrow distribution. The Min-u-sil has approximately 97% of its particles less than 10 μ , the 5 μ Spherisorb has 96% of its particles between 1 μ and 14 μ , and finally, the SiO₂ fume has a very small distribution, with 100% of its particles less than .181 μ .

Scanning electron or transmission electron micrographs are shown for each powder. The Min-u-sil powder, Figure 6, consists of sharp, irregular, slightly agglomerated powders. However, the 5 μ and 10 μ Spherisorb powders, Figures 7 and 8,

*Pennsylvania Glass Sand Corp., Berkeley Springs, W.VA.

**Phase Separatum, Hauppauge, N.Y.

***Provided by Professor P.C. Aitcin, Univ. of Sherbrooke, Canada.

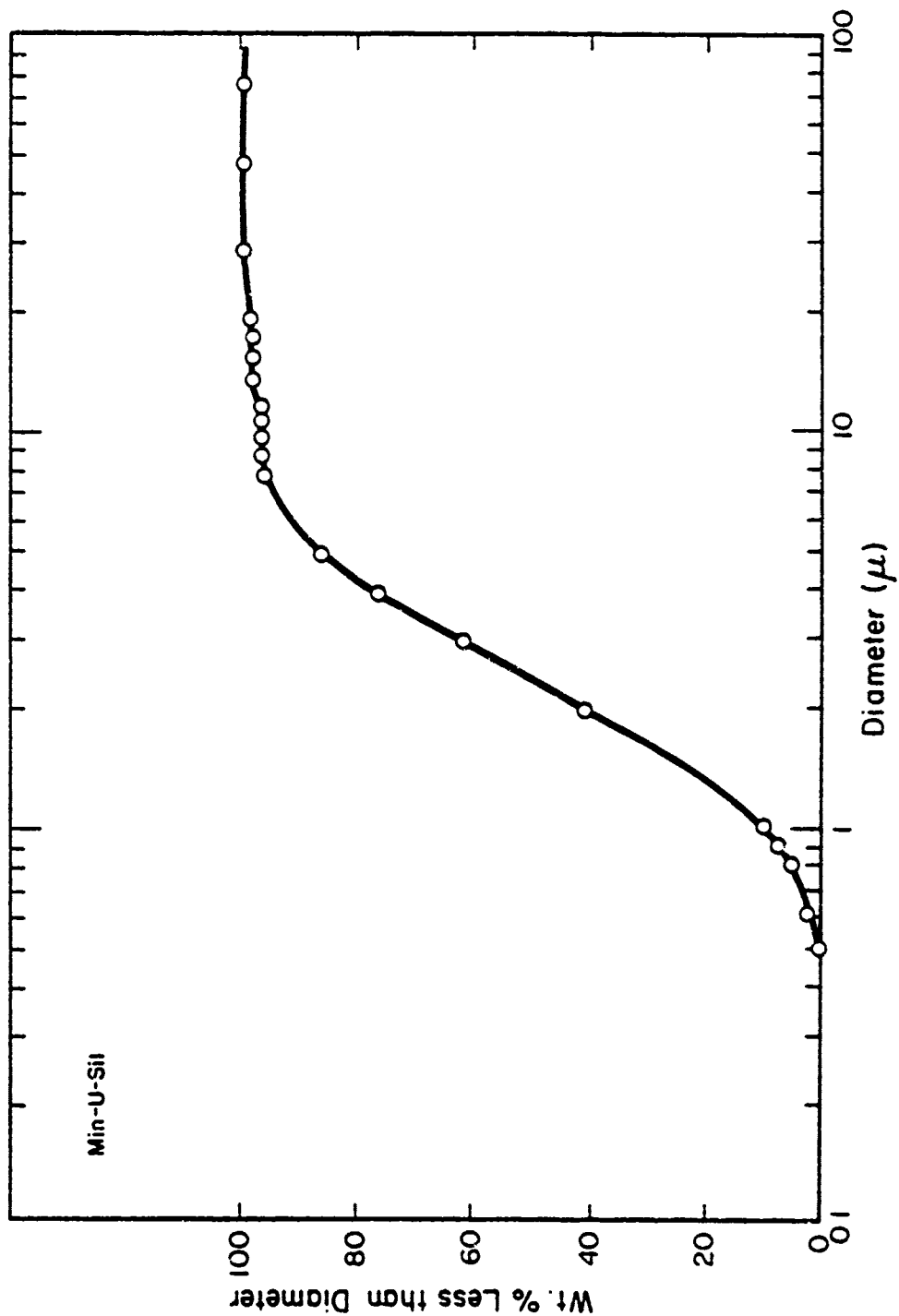


Figure 2. The particle size distribution of the 5μ Min-u-Sil SiO₂.

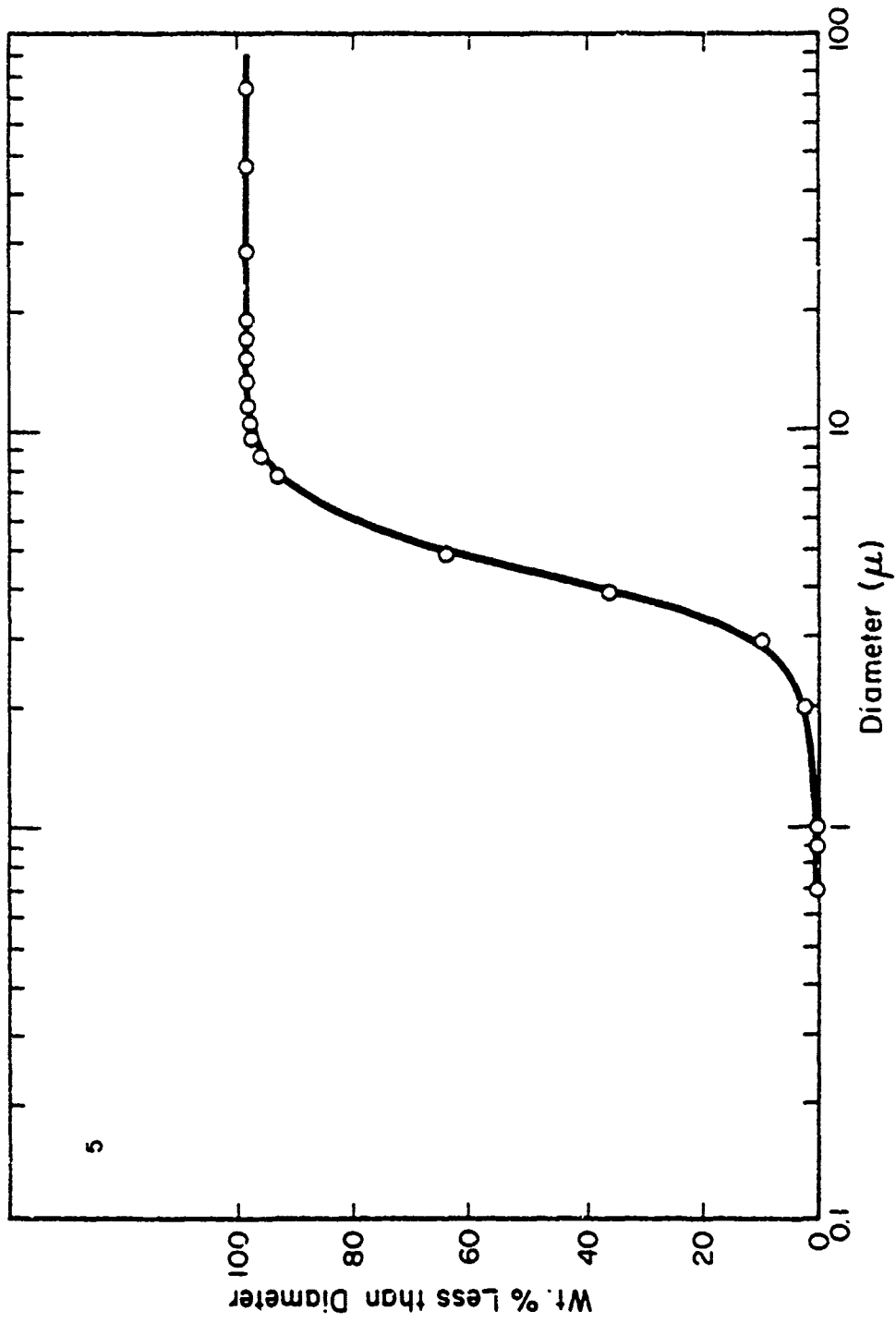


Figure 3. The particle size distribution of the 5μ Spherisorb SiO₂.

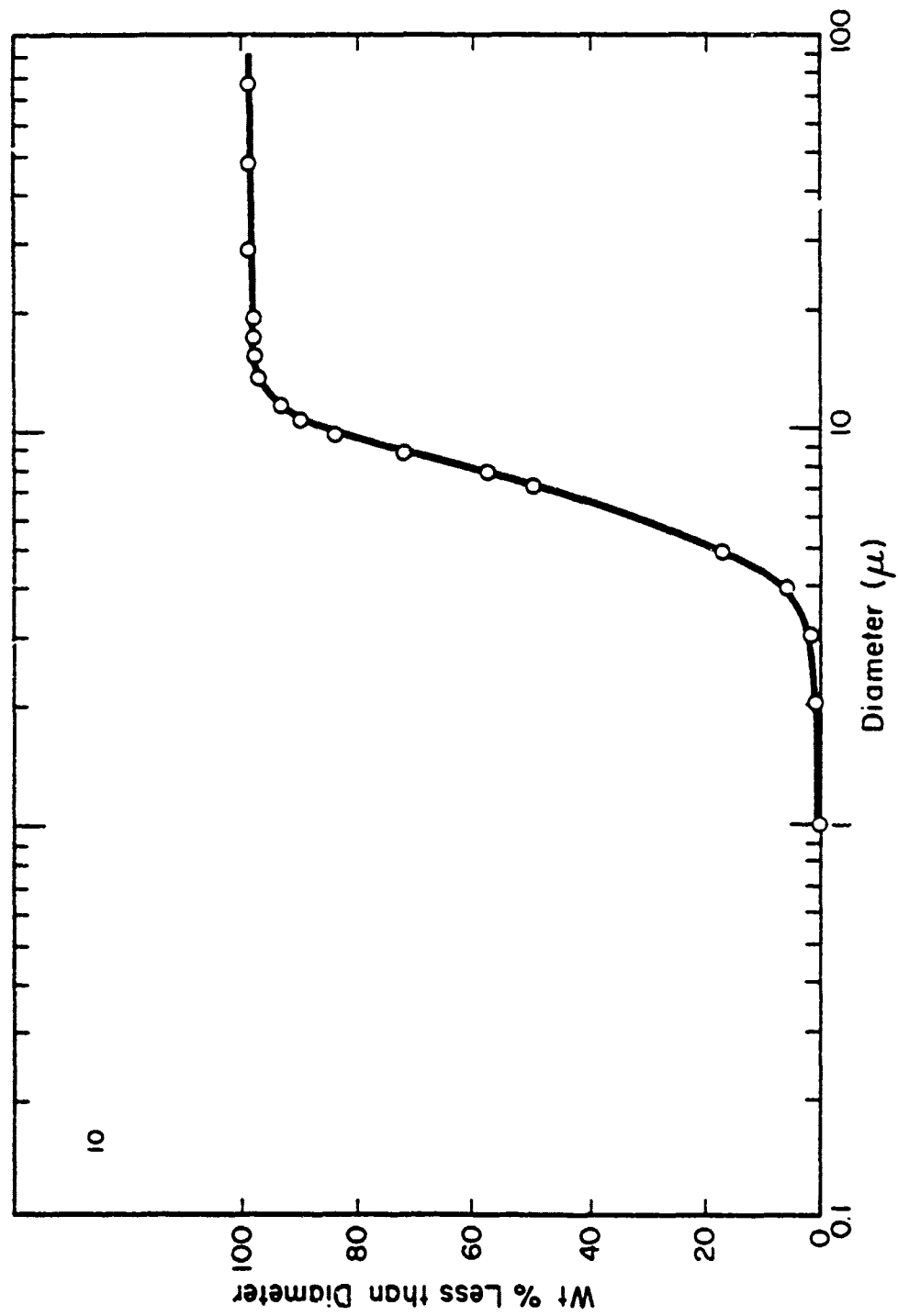


Figure 4. The particle size distribution of the 10μ Spherisorb SiO₂.

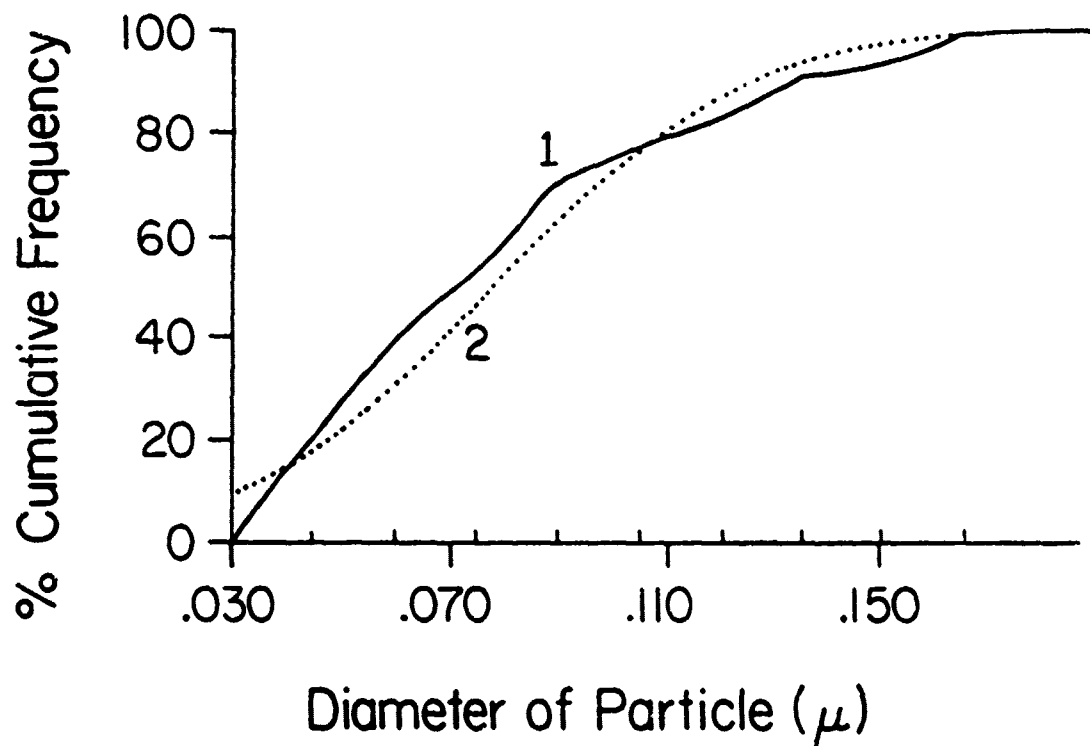


Figure 5. The particle size distribution of the SiO_2 fume. (Curve 1 is the particle size distribution curve, and Curve 2 is a Gaussian best fit distribution of Curve 1.)

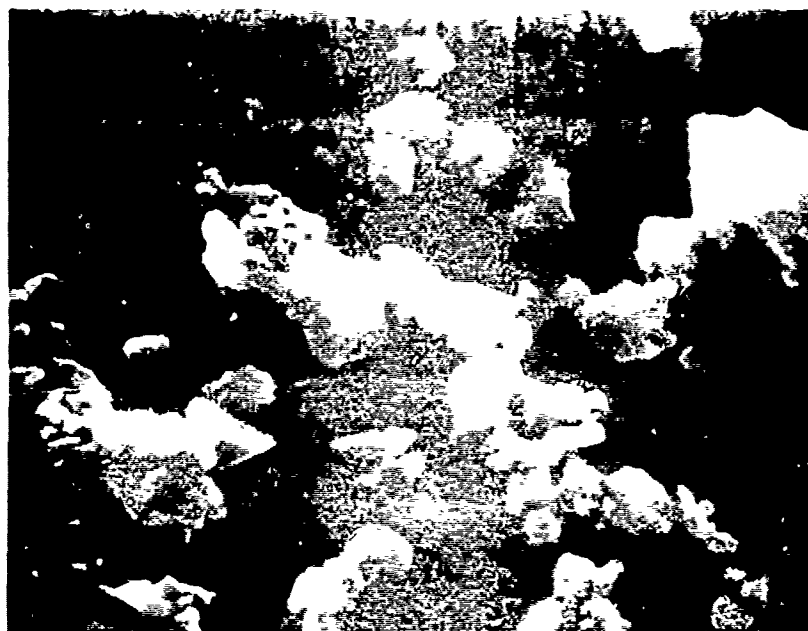
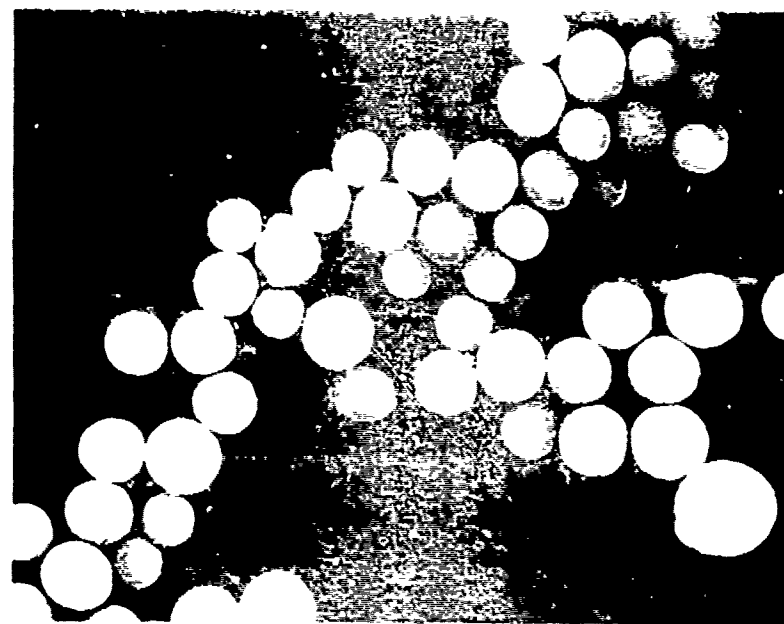


Fig. 1

-S11



Figs.

isorb

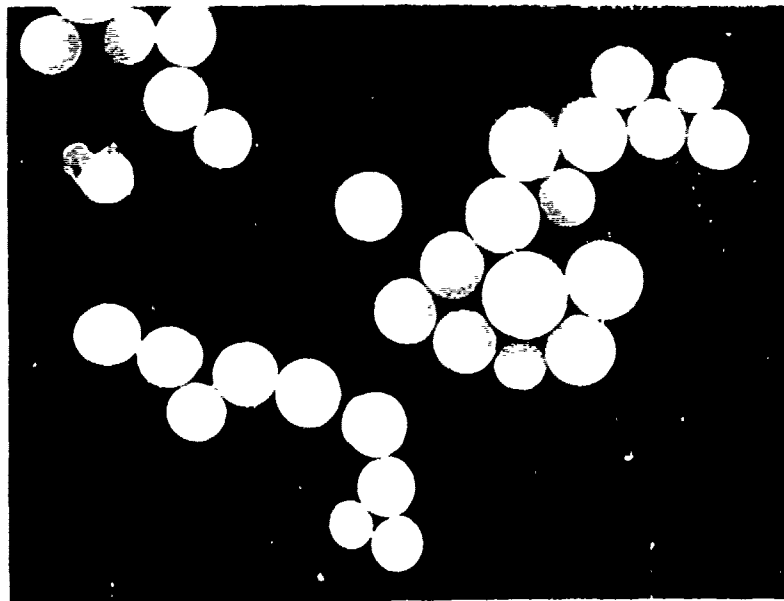


Figure 8. SEM Micrograph of the 10% Spherisorb SiO_2 . 1000X

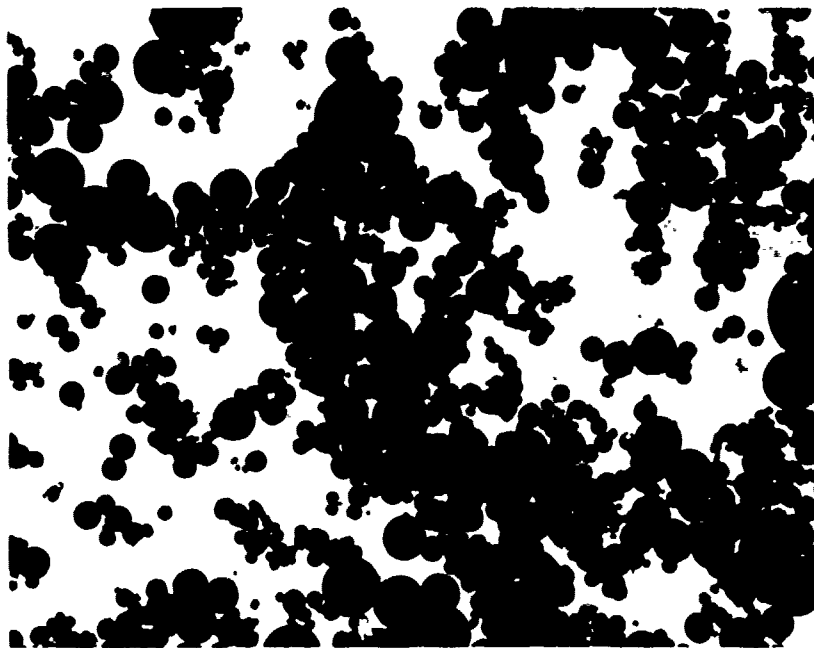


Figure 9. TEM Micrograph of the SiO_2 fume. 76,800X

and the SiO₂ fume, Figure 9, consist of spherical, unagglomerated particles. The 5μ and 10μ Spherisorb SiO₂ were used because of their narrow particle size distributions and the fact that the particles were spherical and unagglomerated. The SiO₂ fume was also studied because of its spherical particles and extremely small size. The Min-u-sil powder was rejected for further study due to the irregular shape of its particles.

b. Spherisorb Powder. An x-ray analysis was performed on the 5μ Spherisorb powder, and the result is shown in Figure 10. A broad peak was found at a 2θ of 22.3°. This corresponds to an amorphous form of silica. No other peaks were observed. A differential thermal analysis was also performed on the 5μ Spherisorb, for two reasons. The first was to check for the release of absorbed or chemical water. The second was to observe how many of the particles were hollow and whether or not a gas was present within them. The results were negative, therefore, no appreciable amounts of adsorbed or chemical water were present. Also, a sample of the heated powder was observed with the SEM to check for evidence of ruptured particles and there appeared to be a larger fraction of broken particles but not significantly so. The specific gravity of the 5 μm Spherisorb was determined by pycnometer. A specific gravity of 2.19 was determined for this powder.

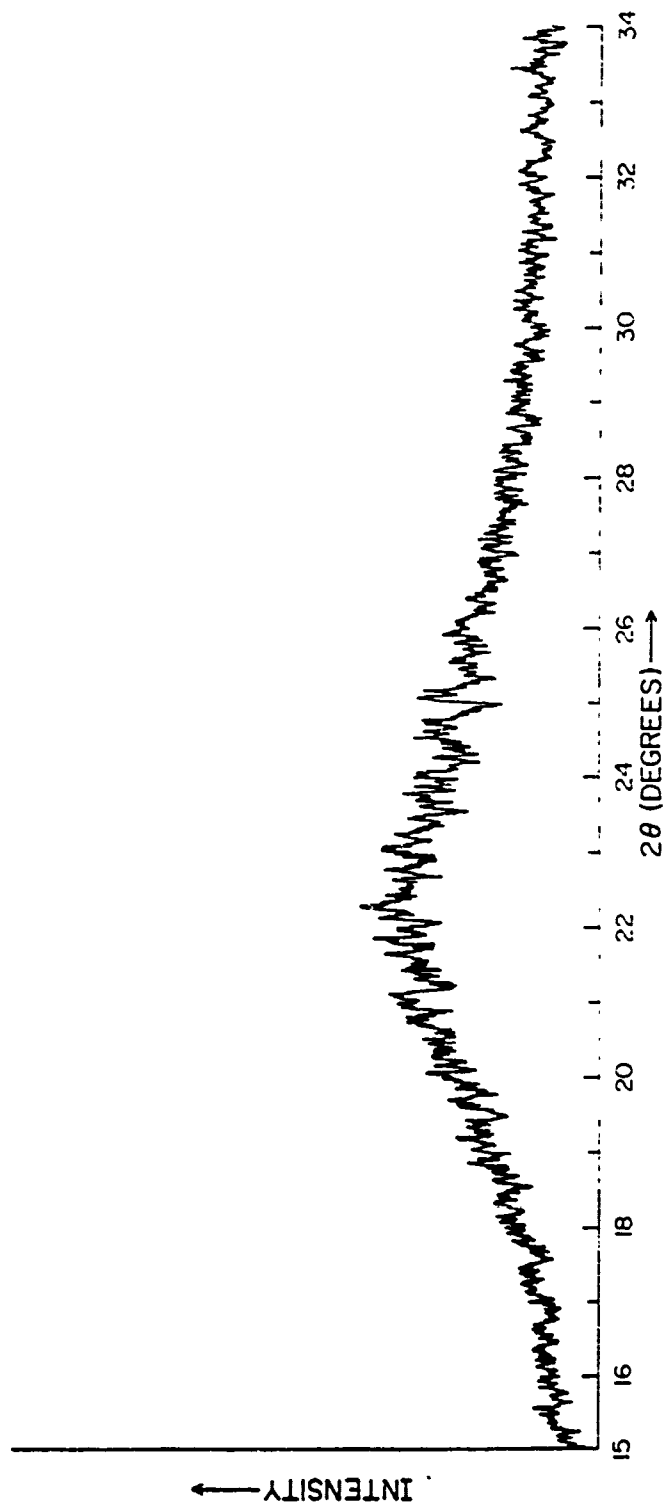


Figure 10. X-ray diffraction pattern of 5μ Spherisorb SiO₂.

c. Fume. The density of the SiO_2 fume was approximately 2.15 gm/cm^3 and is about 95% SiO_2 with the major impurity being carbon.²⁹

2. Casting

a. General. The point of zero charge (zpc) or isoelectric point occurs somewhere between a pH of 1 and a pH of 3.7 for SiO_2 ,^{26,30} The literature seems to support the theory that there is a strong correlation between solubility and the double layer charge.^{31,32} If this is correct, the pH range in which the minimum solubility occurs should be near the isoelectric point for the powder. This is the range in which the minimum dispersion should take place. Therefore, theoretically, the lowest packing densities should occur somewhere within the pH range that gives minimum solubility due to agglomeration. The best packing densities for SiO_2 should therefore occur in the high pH range from 10 to 14.³³

b. Spherisorb Powder. The experimentation began with preliminary tests on the 10μ Spherisorb. These tests included the effect pH had on the centrifugal packing density. One half gram of the 10μ SiO_2 was dispersed in HNO_3 solutions of pH 1 and 3. Each sample was centrifuged at 500, 1000, and 6000 RPM for five minutes. The highest packing density achieved was 26.3% of the theoretical at a pH of 3 for 500 and 1000 RPM.

One gram of the powder was dispersed in pH solution of 2.0, 2.8, 4.8, and 5.6 at 500 RPM for five minutes and the same samples were allowed to settle by gravity. The highest packing density achieved here was 30.4% of the theoretical. This occurred at a pH of 4.8 for both the centrifuged sample and the settled sample. Finally, 1.0 gram of the powder was dispersed in NH_4OH solutions of pH 9.6 and 11.0. The samples were centrifuged at 500 RPM for five minutes, 6000 RPM for five minutes, 6000 RPM for 25 minutes, and allowed to settle by gravity. The highest packing density achieved was 28.5% of the theoretical. This density was achieved with the solution of pH 9.6 with the centrifuged sample (500 RPM), and with the settled sample. The other settled sample, dispersed in a solution of pH 11, also had a 28.5% density. This 10μ powder was then recovered and tested for any detrimental effects brought about by exposure to the acid or base. No significant change in particle size, distribution, or morphology was detected.

After the preliminary tests on the 10μ Spherisorb were completed, the major testing began on the 5μ powder. Only a limited quantity of the 5μ powder was available which precluded a viscosity versus pH experiment. Therefore, the first test attempted was the effect of pH on the centrifugal packing density. The results are shown in Figure 11. Each sample, 1.0 gram of powder

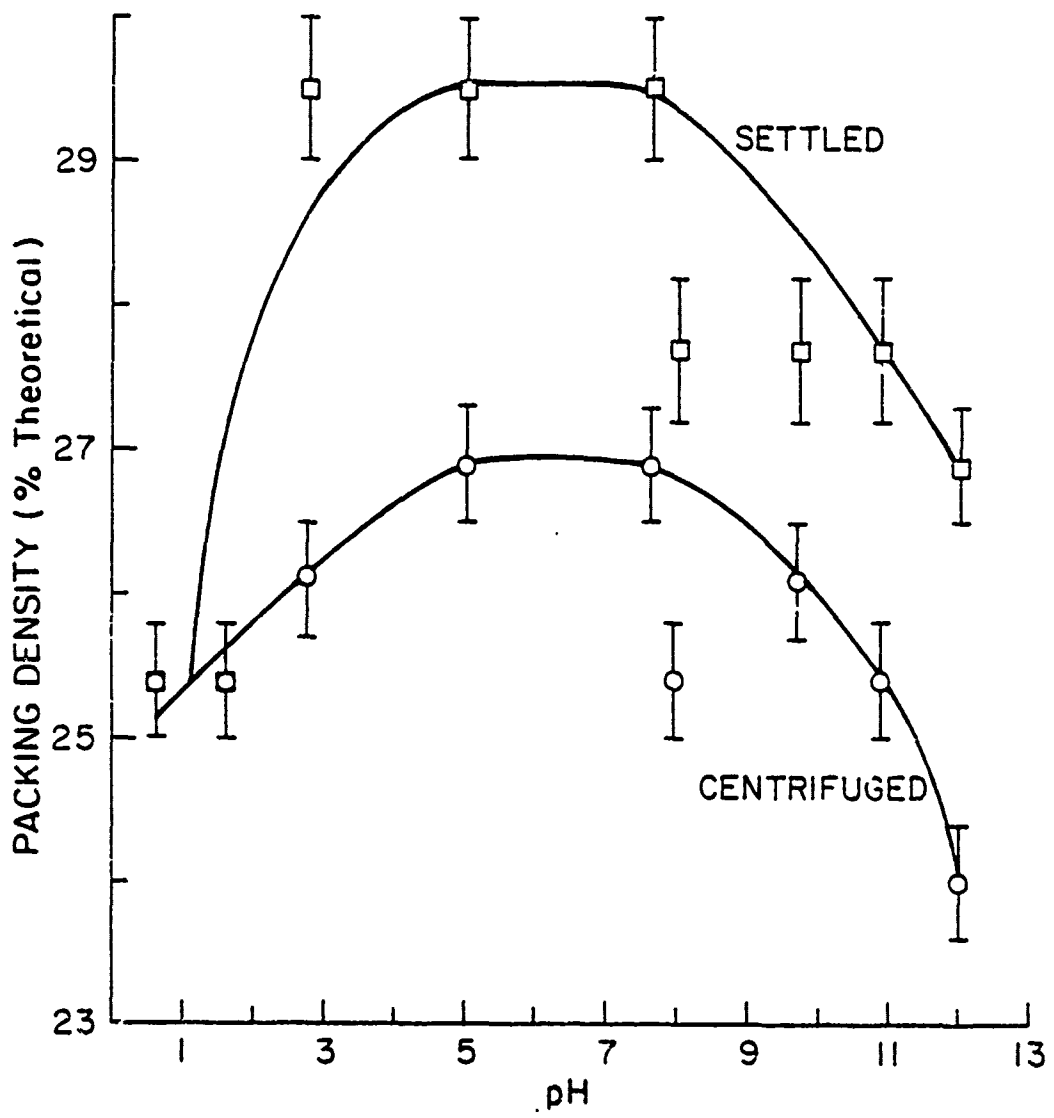


Figure 11. The effect of pH on the centrifugal packing density for the 5 μ Spherisorb SiO₂.

dispersed in pH solutions of .6-12 (using HNO_3 and NH_4OH), was centrifuged at 6000 RPM for various times. The powder was also allowed to settle by gravity. In Figure 11, a pattern appears. For the centrifuged sample, the packing density increases from pH 1-5 and then decreases from pH 7.6-12, with the highest density, 26.9% of the theoretical, occurring at a pH of 5 and 7. The curve for the settled sample shows the same trend; however, the packing densities are higher. The peaks occur at the same pH value, but the density is 29.5%. This curve shows two interesting phenomena. First, the slower settling powder gave the higher packing densities. Secondly, the packing density decreased from pH 7-12. The error bars correspond to the inaccuracy associated with reading the packing volumes from the graduated test tubes. The packing volume could be determined within $\pm .3$ ml.

A 1.0 gram sample of the 5u powder was dry packed in a tube. This was accomplished by submitting the tube to an ultrasonic bath after the addition of the powder. The packing density achieved was 22.8% of the theoretical. This value is similar to the densities obtained by centrifugal slip casting.

Table 1 shows centrifugal packing densities achieved for different dispersants and different concentrations of these dispersants. The highest packing density achieved

Table 1. Centrifugal Packing Density as a Function of Dispersant for 5% SiO₂

Dispersant & Concentration	Centrifuging Speed (RPM)	Centrifuging Time (min.)	Packing Volume (cm ³)	Packing Density (% Theor.)
HF 2 drops/100 ml H ₂ O	5000	4	1.80	25.4
2 drops/100 ml H ₂ O	6000	5	1.80	25.4
1.3 drops/15 ml H ₂ O	6000	5	1.80	25.4
1 ml/13 ml H ₂ O	500	10	1.50	30.4
1 ml/13 ml H ₂ O	7500	5	1.60	28.5
1 ml/13 ml H ₂ O	7500	10	1.50	30.4
1 ml/13 ml H ₂ O	7500	30	1.60	28.5
HNO ₃ pH=2+1 drop				
Darvan #7	5000	4	1.80	25.4
pH=2+2 drops				
Darvan #7	6000	5	1.80	25.4
NH ₄ OH pH=11+1 drop				
Darvan #7	5000	4	1.80	25.4
pH=11+2 drops				
Darvan #7	6000	5	1.80	25.4
Aceton 1	5000	4	1.80	25.4
Aceton 2	6000	5	1.80	25.0
Sodium Silicate				
1 drop/14 ml H ₂ O	Settle by gravity		1.70	26.9
1 drop/14 ml H ₂ O	7500	15	1.90	24.0
.5 ml/14 ml H ₂ O	settle by gravity		1.70	26.9
.5 ml/14 ml H ₂ O	7500	15	2.00	22.8
Potassium silicate				
1 drop/14 ml	settle by gravity		1.60	28.5
1 drop/14 ml	7500	15	1.80	25.4
Tri-sodium phosphate				
1 drop/14 ml	Settle by gravity		1.70	26.9
1 drop/14 ml	7500	15	1.90	24.0
Mighty 150 10 ml/30 ml H ₂ O	7500	20	1.90	24.0
1 ml/100 ml H ₂ O	7500	20	1.90	24.0
Melment L10 10 ml/10 ml H ₂ O	7500	20	1.90	24.0
1 ml/100 ml H ₂ O	7500	20	1.90	24.0

was 30.4%. This was accomplished using an HF-H₂O solution, 7.7% HF by volume, and centrifuging at speeds of 500 and 7500 RPM.

The results of centrifugal packing density with the concentration of powder are shown in Figure 12. The data again show that the powders settled by gravity gave higher packing densities than the centrifugally cast powder. The data also show that above 1.0 gram of powder, the packing density increased with increased powder content. The dispersant used was an NH₄OH solution of pH = 10.

Since the packing density appears to depend on settling time, a packing density study as a function of the viscosity of the settling medium was performed. The settling time is directly proportional to the viscosity. Therefore, increased viscosity implies increased settling time. One half gram of 5 μ m SiO₂ was dispersed in different glycerine-H₂O mixtures (0%, 25%, 50%, and 75% glycerine by volume), and allowed to settle. The results are shown on Figure 13. There is an increase in density with increasing viscosity, up to 6.05 centipoise, and then a decrease.

Finally, Figures 14 and 15 show the microstructure of the centrifugally slip cast 5 μ m Spherisorb SiO₂. These photographs were obtained on fracture surfaces to avoid possible misleading results that might occur at the slip, free surface interface. The micrographs show a random

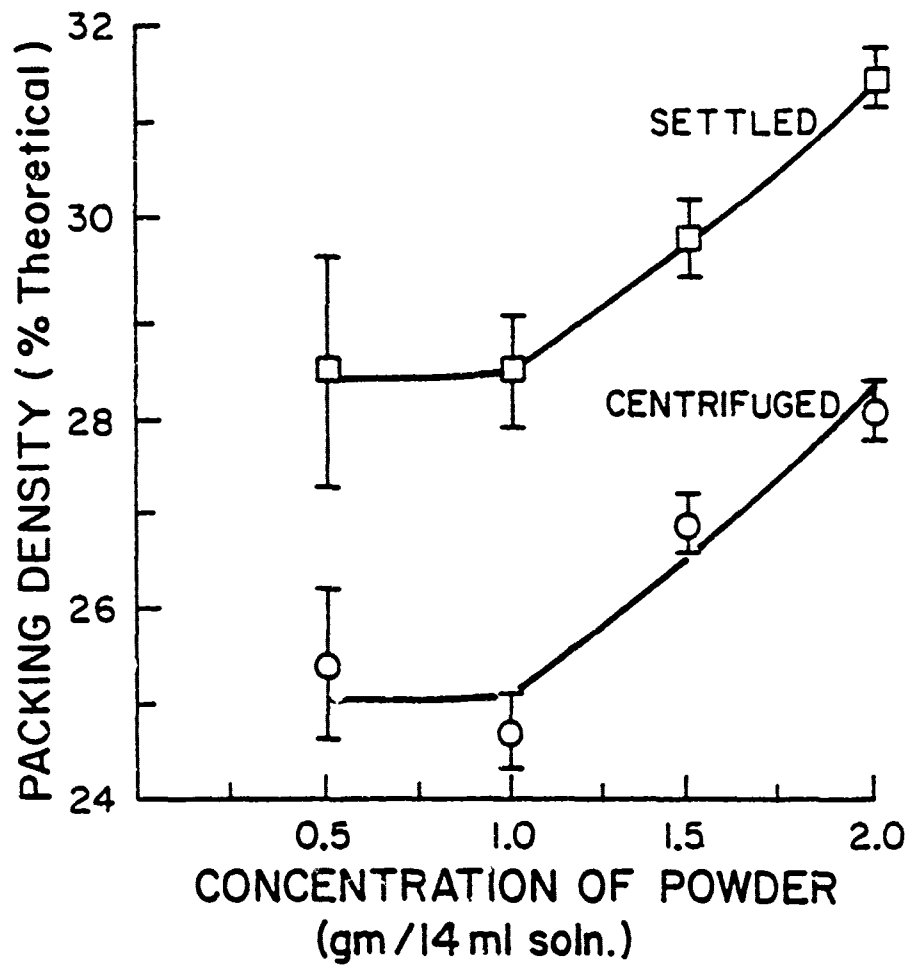


Figure 12. The effect of the concentration of powder in the slip on the centrifugal packing density of the 5 μ Spherisorb SiO₂.

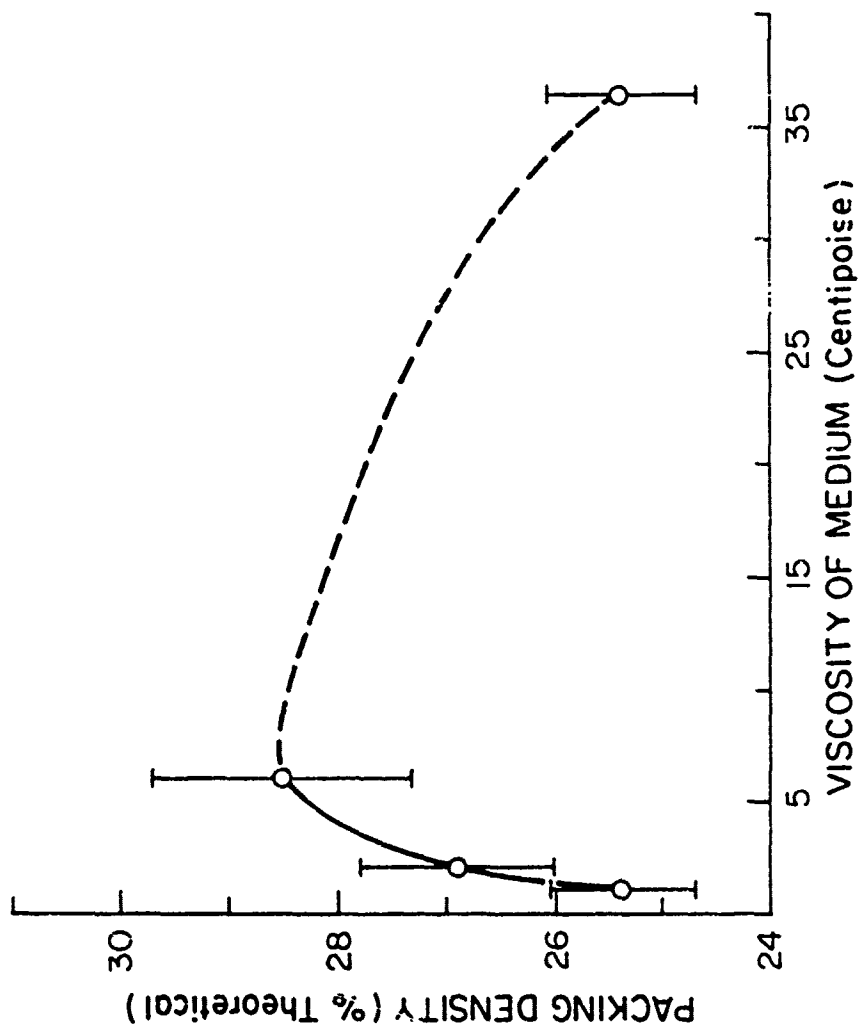


Figure 13. The effect of the viscosity of the settling medium on the packing density of the 5 μ Sphaerisorb SiO₂.

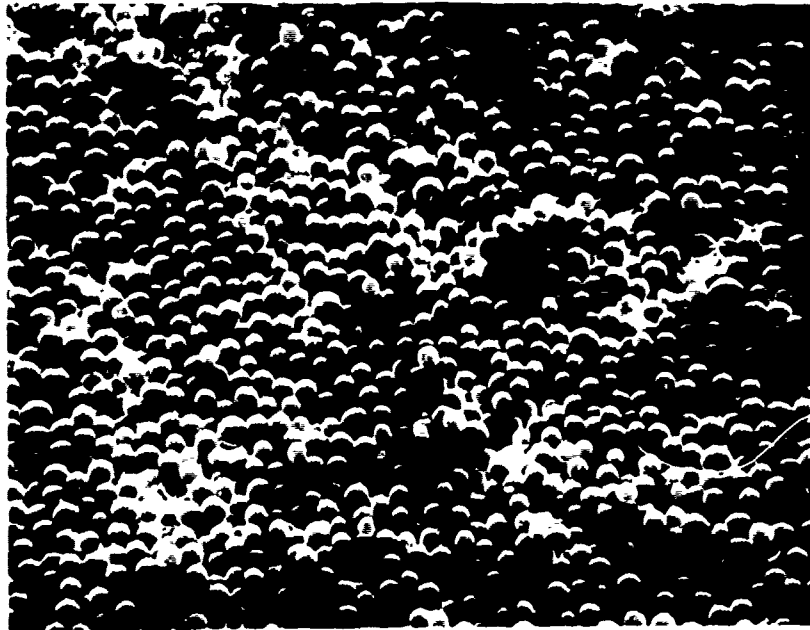


Figure 14. SEM Micrograph of a packing of the 5% Spherisorb SiO_2 . 368X

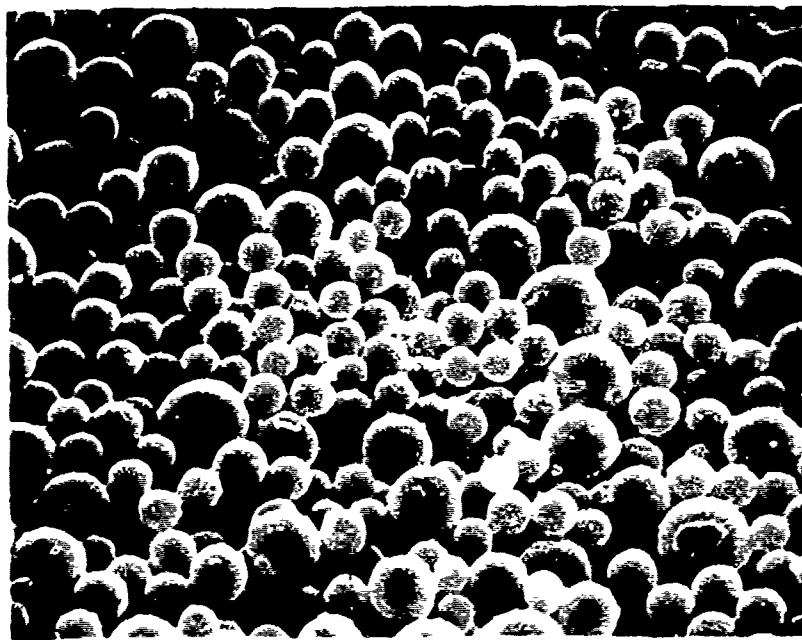


Figure 15. SEM Micrograph of a centrifugally cast packing of the 5% Spherisorb SiO_2 . 700X

packing of the particles. The smaller particles seem to pack more uniformly but the larger particles seem to disrupt the packing. Pellets were centrifugally cast for density measurements. However, they had no green strength when dried and measurements could not be made.

The best centrifugal packing density achieved with the 5 μ Spherisorb was 30.4% of the theoretical. The low density and the microstructure show that close packing was definitely not achieved. There could be a number of reasons for this and will be discussed later.

c. Fume. Centrifugal packing density was measured using 1.0 gram of the powder dispersed in the feeding solution described earlier. The packing density achieved was 38.8% of the theoretical. The as-received powder did contain some agglomerates which would not disperse. Therefore, these were allowed to settle as described earlier, and the fines collected. The fines were then used for a second centrifugal packing study. Again 1.0 gram of the powder was dispersed in three different dispersants, Mighty 150, Melment L10, and feeding solution. These samples were then centrifuged at 6000 RPM for approximately 75 minutes. The packing densities achieved were 51.7% of the theoretical for the Mighty 150, 51.7% for the Melment L10, and 58.1% for the feeding solution.

A centrifugally cast pellet was fabricated at 11,000 RPM, however, it cracked during drying. Therefore, a density measurement could not be performed on a dry pellet. A piece of a pellet centrifuged at 7500 RPM was studied under the SEM, and Figure 16 shows the structure. Again, a random packing is observed.

B. ZnO

1. Powder Characterization

Four different ZnO powders were examined. Their particle size distributions are shown in Figures 17-20. Approximately 96% of the Baker* Reagent grade ZnO particles are less than 12 μm . St. Joe's #17 has approximately 96% of its particles less than 8 μm , St. Joe's #30 has approximately 96% of its particles less than 5 μm , and St. Joe's #100 has approximately 96% of its particles less than 6 μm . All of these powders had distributions suitable for these experiments.

Figure 21 is an SEM micrograph of the Baker Reagent ZnO. This powder, consisting of small, irregularly shaped agglomerates, was unsuitable for the casting experiments. Figure 22 shows the typical shape of all the St. Joe ZnO

* J.T. Baker Chemical Co., Phillipsburg, N.J., Lot No. 39540.

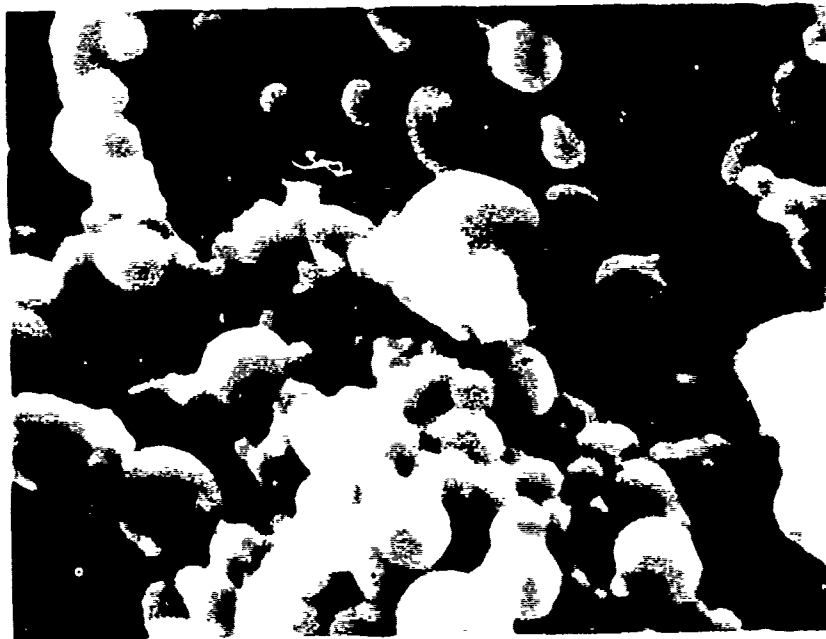


Figure 16. SEM Micrograph of a centrifugally cast packing of the SiO₂ fume.
48,000X

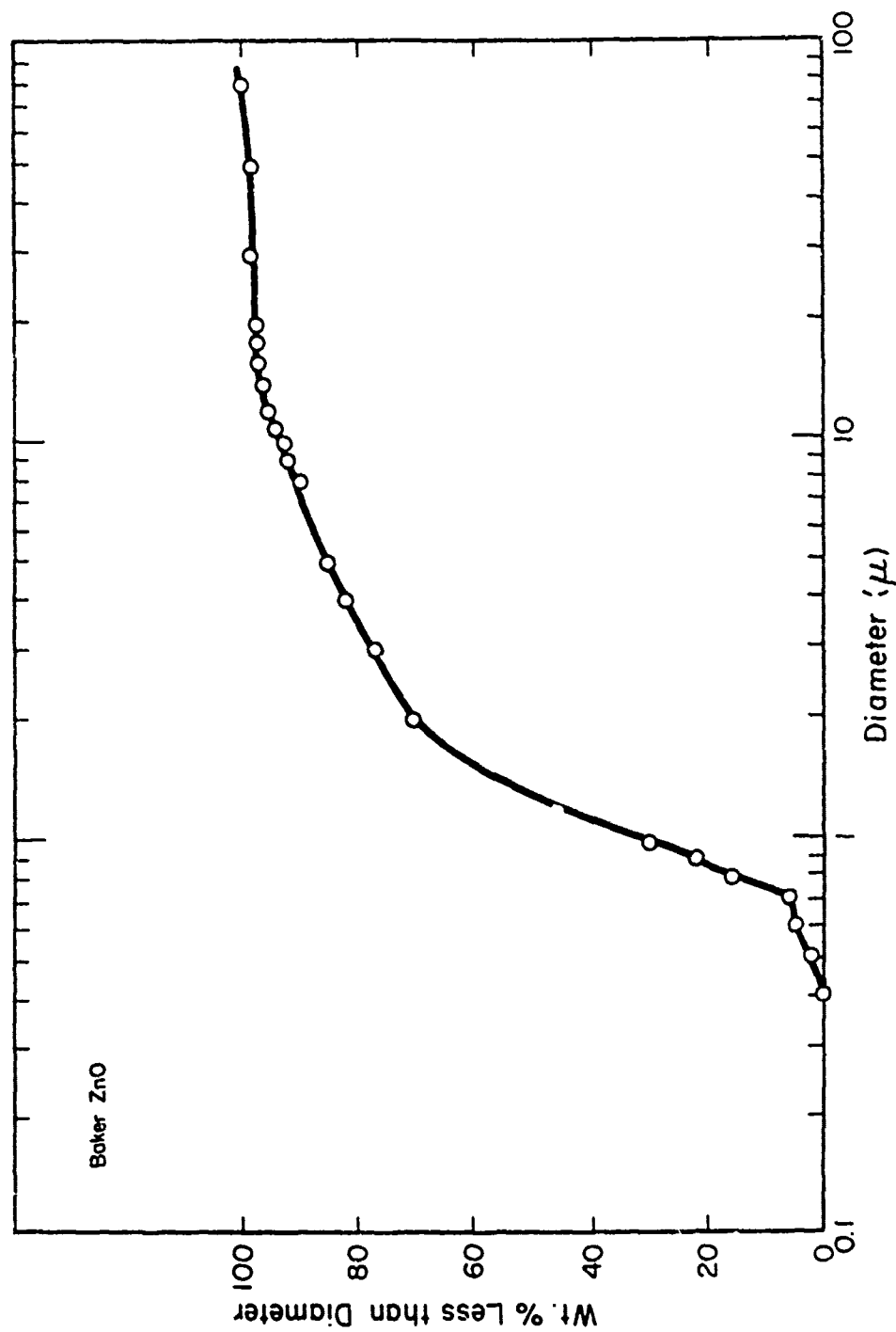


Figure 17. The particle size distribution of the Baker Reagent ZnO.

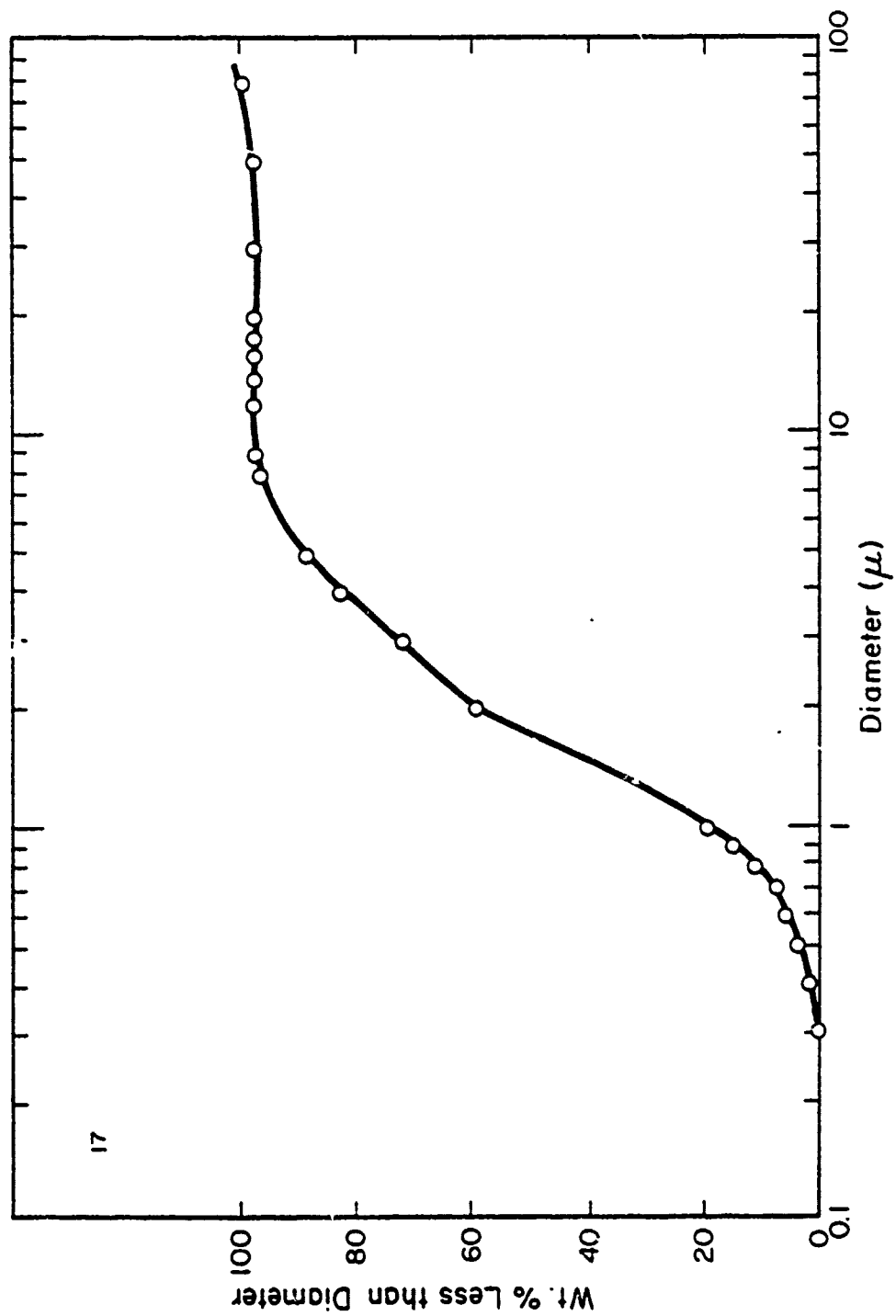


Figure 18. The particle size distribution of the St. Joe's #17 ZnO.

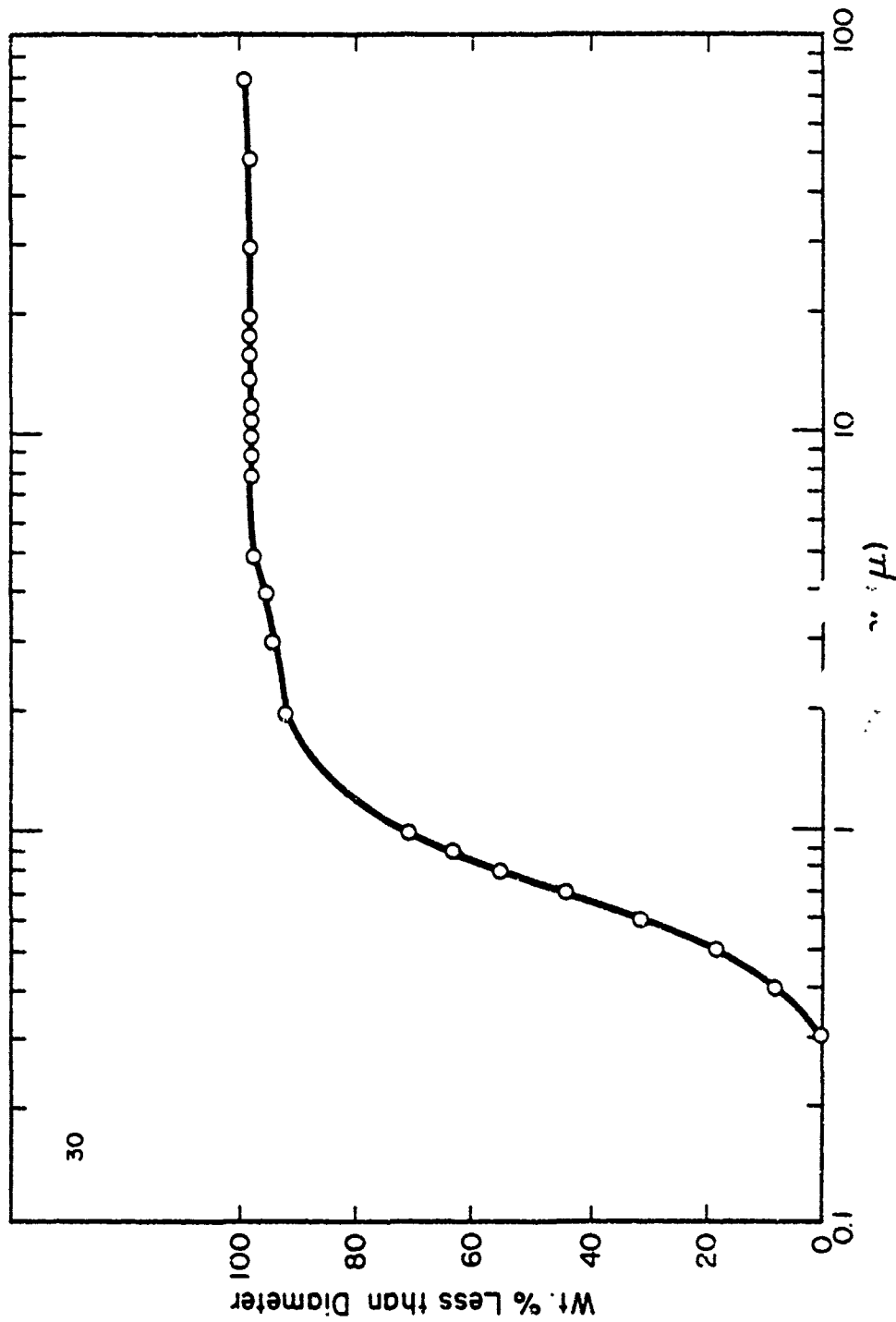


Figure 19. The particle size distribution of the St. Joe's #30 ZnO.

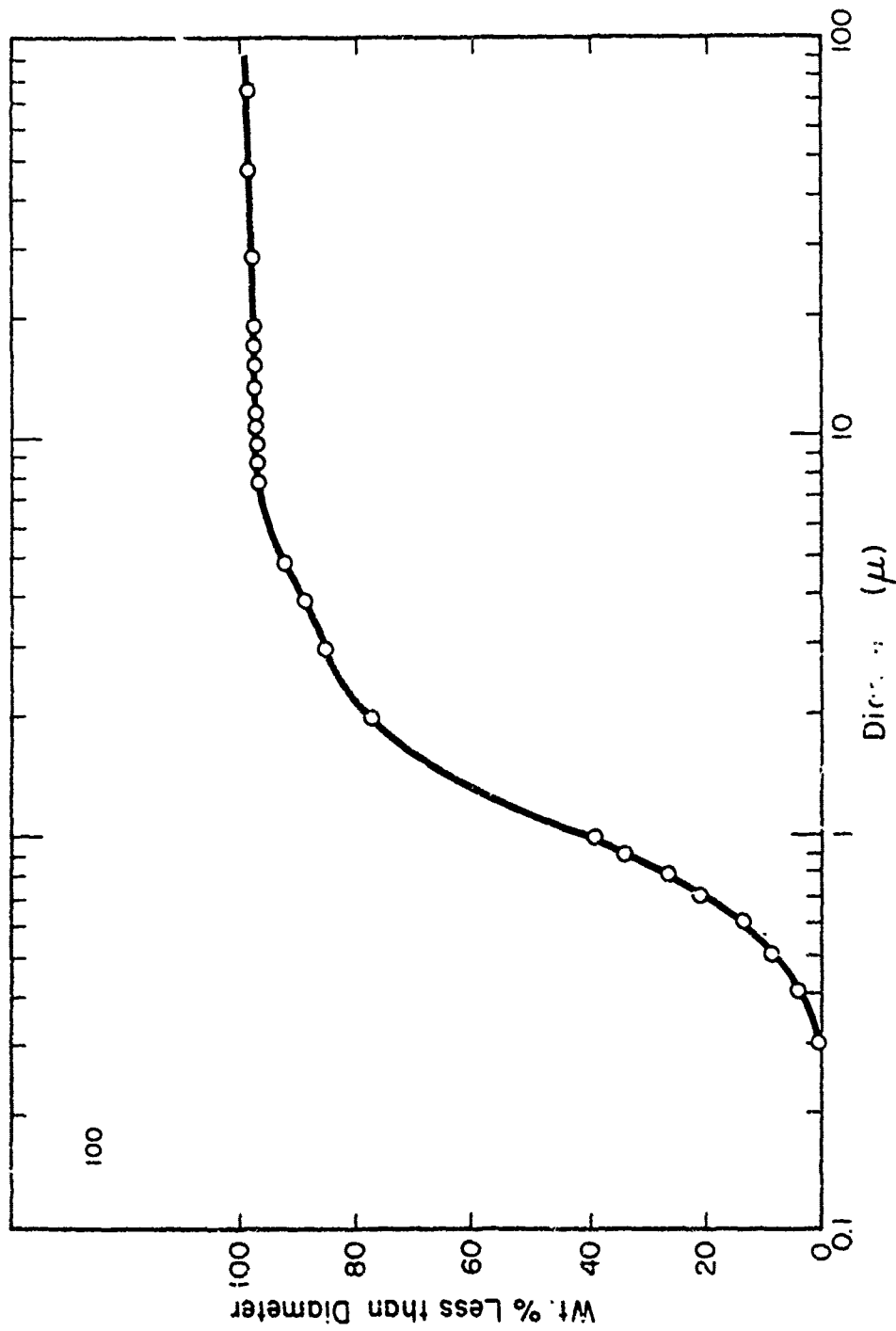


Figure 20. The particle size distribution of the St. Joe's #100 ZnO.

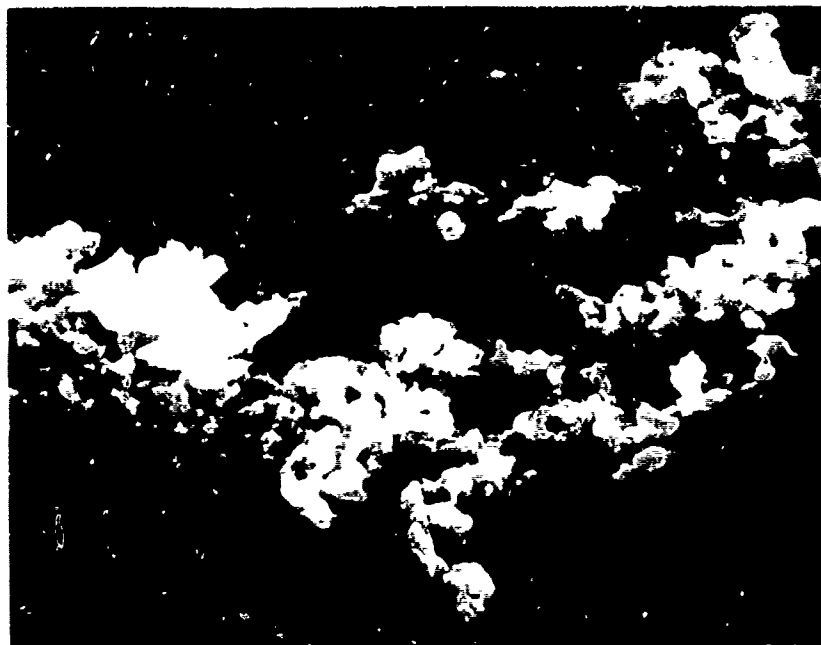


Figure 21. SEM micrograph of the Parker Reactant ZnO. 7000X



Figure 22. TEM Micrograph of the St. Joe's #100 ZnO. 23,200X

powders. This TEM micrograph is of the #100 ZnO, but represents the irregular particle shapes of all the St. Joe ZnO. All of these powders had acceptable particle size distributions; however, none of them had an acceptable particle shape. Therefore, because of the lack of a better ZnO powder to work with, and because there was an abundance of it, the St. Joe #100 ZnO was used for the centrifugal packing density studies.

2. Viscosity versus pH

Again there seems to be a correlation between the solubility of ZnO and its double layer charge.³⁴ The zero point of charge for ZnO occurs between a pH of 8 and 9^{34,30} and the solubility minimum occur at a pH of about 9. Therefore, it is expected that a maximum slip viscosity would occur at a pH of 9 and decrease with an increase or decrease in pH.

The effect of pH on the viscosity of a ZnO slip was measured with a Brookfield viscometer, using spindle 3 and a speed of 20 RPM. Two trials were performed on slips that consisted of an 8-9% solids content by volume. Figure 23 gives the result of one of these viscosity versus pH experiments. This result is not what was expected based on the literature data on solubility. Instead of a maximum viscosity at a pH in the neighborhood of 8-10, a minimum is observed. Part of this is probably due to the fact that

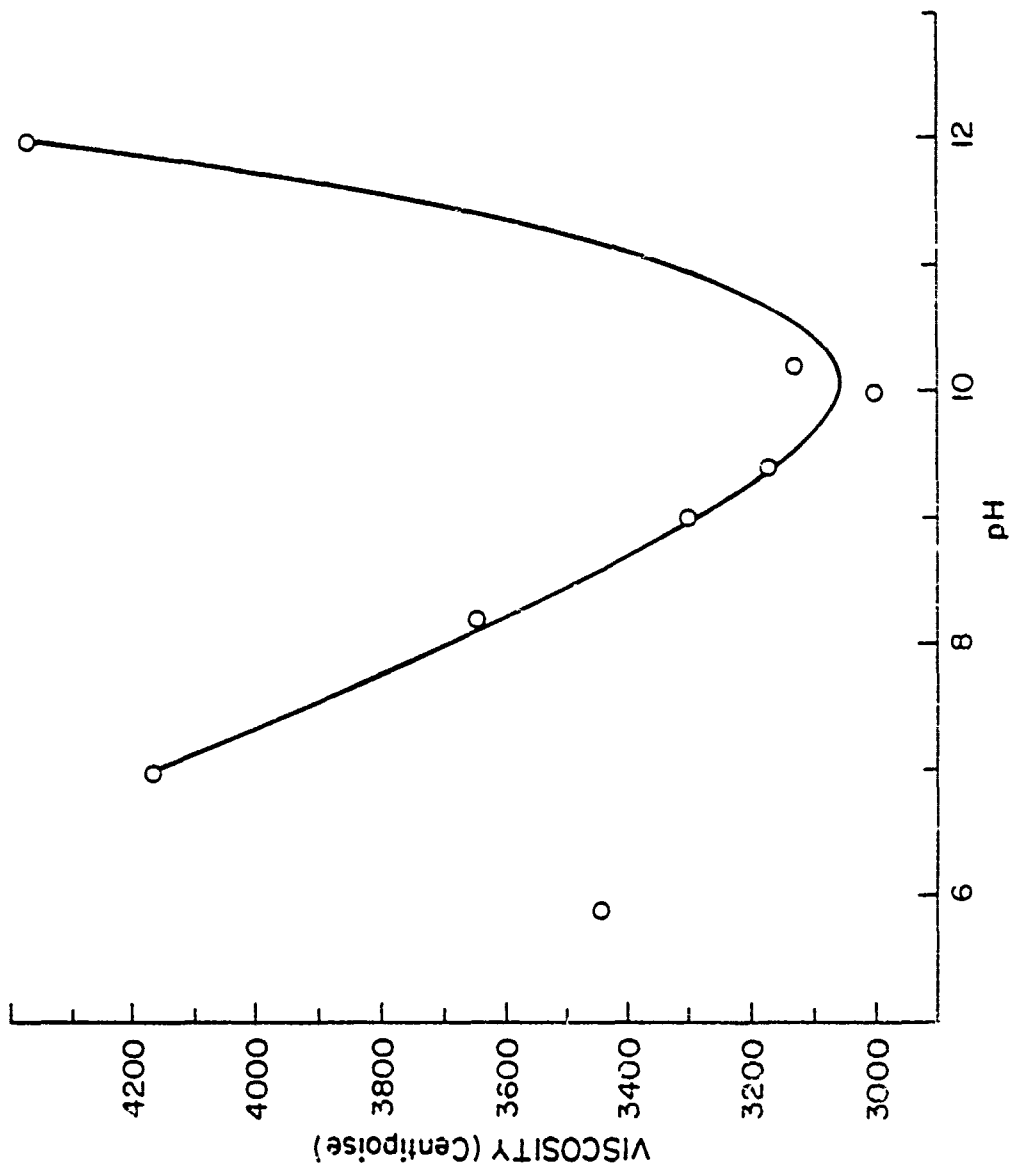


Figure 23. The effect of pH on the viscosity of the slip for the St. Joe's #100 ZnO - Trial 2.

the ZnO described rather quickly in the acidic solutions and pH values below 9.0 were unstable. It should be noted that that lone data point at pH6 was reproduced in both experiments and may represent a rapidly changing pH due to the low initial pH.

3. Casting

a. As-received Powder. The effect of pH on the centrifugal packing density is shown in Table 2. For each sample, 2.0 grams of powder were dispersed in HNO₃ or NH₄OH solutions and centrifuged a 6000 RPM for 10-15 minutes. The highest density achieved was 31.0% of theoretical at a pH of 12. Table 2 clearly shows the pH instability of the acidic solutions which casts serious doubt on the validity of the viscosity versus pH data. This is exemplified by the fact the packing density versus pH is what is expected from solubility and zero point of charge data and is opposite to the viscosity data. As a result, further runs were performed only a high and stable pH values. The effect of concentration of powder in the slip on the packing density was determined and are shown in Figure 24. An NH₄OH solution of pH 10 was used as the dispersant, and the suspensions were centrifuged at 7500 RPM for 15 minutes. Although the data are scattered, there is an increase in packing density with an increase in the powder concentration. The highest density obtained was 36.9%.

Table 2. pH vs Centrifugal Packing Density
for St. Joe's #100 ZnO - Trials 1
and 2.

6000 RPM for 10 minutes

Starting pH	Packing Volume (cm ³)	Packing Density (%Theor.)	Packing Volume (cm ³)	Packing Density (%Theor.)	Final pH
.60	1.20	29.7	1.00	35.7	6.20
1.60	1.40	25.5	1.10	32.4	7.10
2.75	1.40	25.5	1.20	29.7	9.10
3.80	1.40	25.5	1.25	28.5	9.70
5.00	1.40	25.5	1.15	31.0	9.90
5.75	1.40	25.5	1.20	29.7	10.00
6.00	--	--	--	--	--
8.00	1.40	25.5	--	--	--
9.00	1.40	25.5	1.35	26.4	10.00
9.70	1.35	26.4	1.15	31.0	10.00
10.90	1.25	28.5	1.15	31.0	10.60
12.00	1.15	31.0	1.00	35.7	12.35

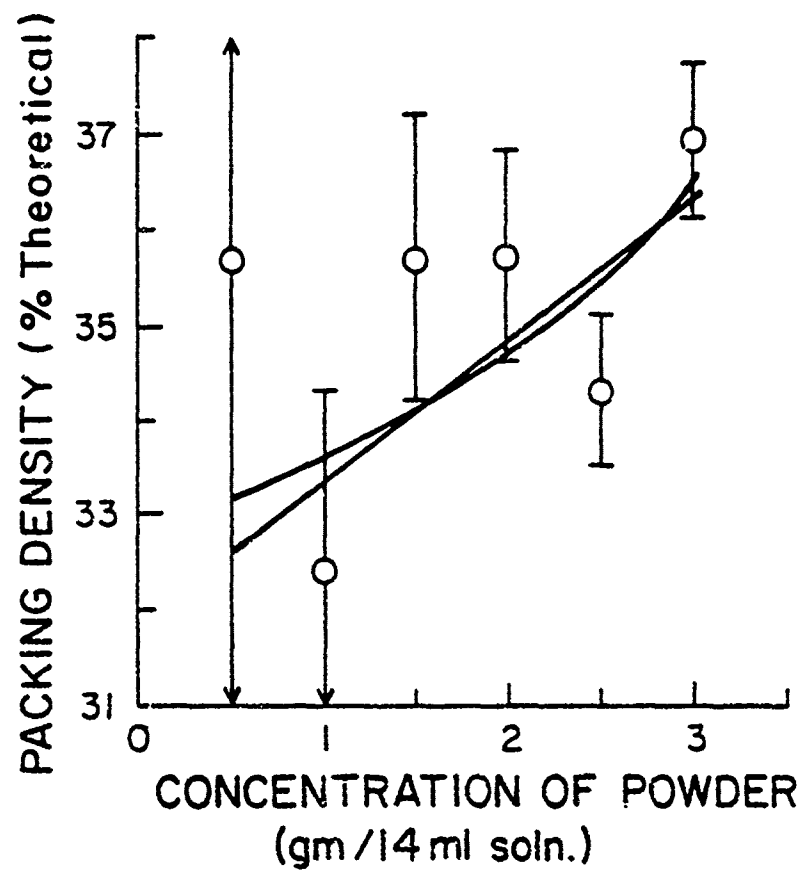


Figure 24. The effect of the concentration of powder in the slip on the centrifugal packing density of the St. Joe's #100 ZnO.

b. Fines Only. To observe low packing density varied with particle size, the particle size distribution was changed by removing particles 1 μ m and above by settling as described earlier. Packing density was measured only in the pH range from 10-12. Again, each sample consisted of 2.0 grams of dispersed powder that was centrifuged at 7500 RPM for 60 minutes. The results are tabulated in Table 3. A 35.7% packing density was achieved with the solutions of pH 10 and 11, and the solution of pH 12 gave a 32.4% packing density. Again, it appears as if higher packing densities are achieved with smaller particles.

Different dispersants were also used to disperse 2.0 grams of the ZnO fines to observe if the packing density could be increased. Centrifuging took place at 7500 RPM for 60 minutes. The results are shown in Table 4. The feeding solution, sodium silicate, and potassium silicate all gave packing densities of 35.7%, and tri-sodium phosphate gave a 32.4% of the theoretical packing density, all of which are no improvement.

It was discovered that sound centrifugally cast pellets could be made from the ZnO powder that contained 1 μ or less particles. The powder, usually 2.0 grams, was dispersed in an acid or base solution, and centrifuged in a round bottom test tube (the graduated test tubes were conical in shape), at 11,000 RPM. The liquid was then decanted, and

Table 3. pH vs Centrifugal Packing Density for St. Joe's #100 ZnO, (Particle Size <math><1\mu</math>).

Approx. pH	Packing Volume (cm ³)	Packing Density (%Theor.)
10.0	1.00	35.7
11.0	1.00	35.7
12.0	1.10	32.4

Table 4. Centrifugal Packing Density as a Function of Dispersant for St. Joe's #100 ZnO (Particle Size <math><1\mu</math>).

Dispersant & Concentration	Speed of Centrifuging (RPM)	Time of Centrifuging (min.)	Packing Volume (cm ³)	Packing Density (%Theor.)
Feeding Solution	7500	60	1.00	35.7
Sodium Silicate (1 drop/14ml H ₂ O)	7500	60	1.00	35.7
Potassium Silicate (1 drop/14ml H ₂ O)	7500	60	1.00	35.7
Tri-Sodium Phosphate (1 drop/14ml H ₂ O)	7500	60	1.00	32.4

the pellet was allowed to slowly dry. Fast drying caused surface cracking. When dry, the pellet was removed from the test tube, intact. The density of one of these centrifugally cast ZnO pellets that was dispersed in an NH_4OH solution of pH 10, was 44.5% of theoretical.

c. Ball-milled Powder. Finally, in an attempt to lower the particle size distribution and break up some of the irregularly shaped particles, the powder was dry ball milled in a polyethylene container with high alumina balls for 6-1/2 hours and then wet ball milled 5-1/2 hours more. Figure 25 shows the particle size distribution of the powder after ball milling. The distribution has shifted to smaller sizes, as compared to the original powder. Now 96% of the particles are less than 4μ , instead of 6μ , and this powder contains more fines. 5-1/2 more hours of ball milling, wet, did not change the distribution appreciably. A TEM micrograph, Figure 26, shows that a number of the irregular particles were broken up, but there are still a large number intact.

A sample of the ball-milled ZnO was dispersed in the feeding solution and centrifuged to a density of 39.6% which is a minor improvement of that of the unmilled material.

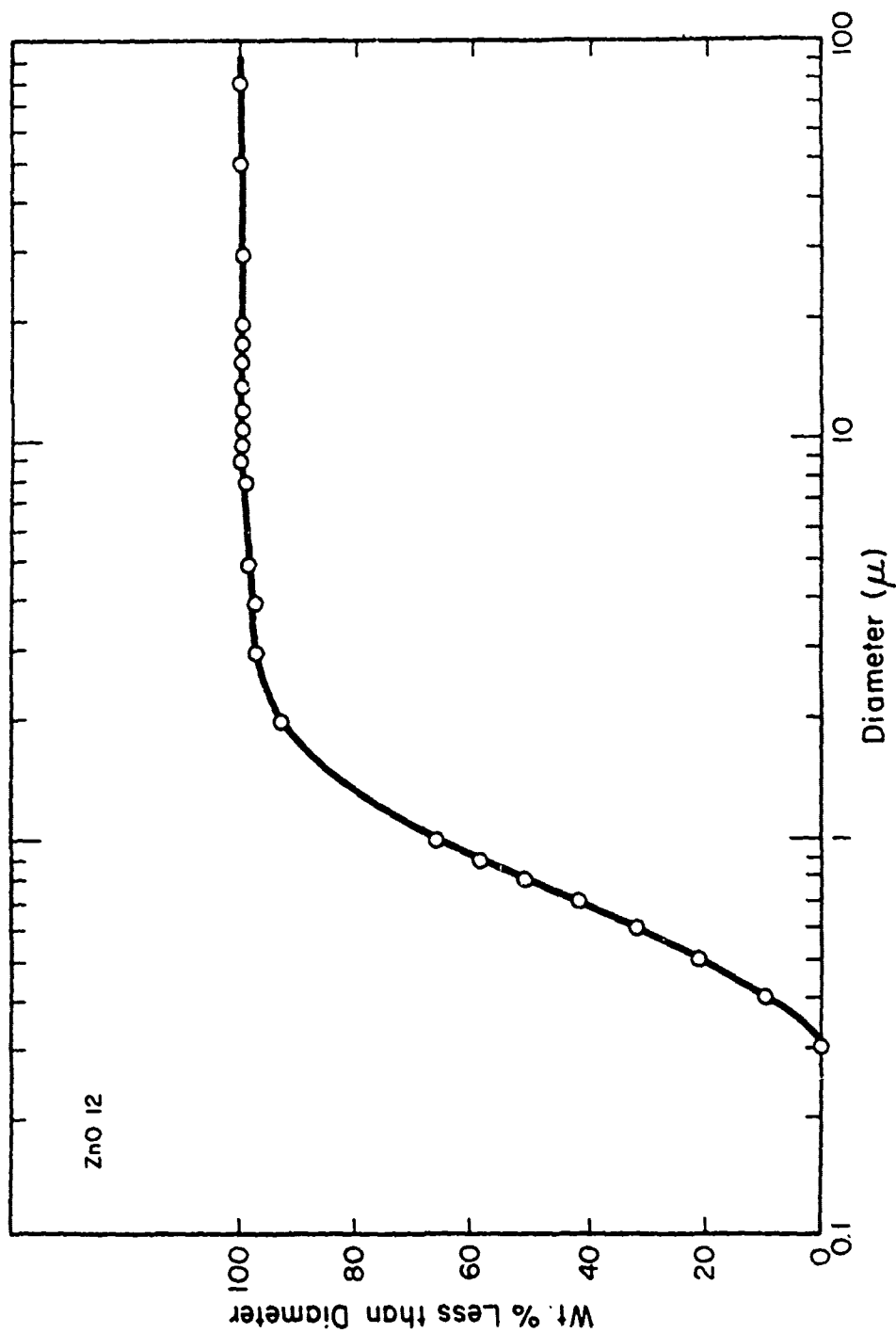


Figure 25. The particle size distribution of the St. Joe's #100 ZnO that was dry ball milled 6½ hours and then wet ball milled for 5½ more hours.

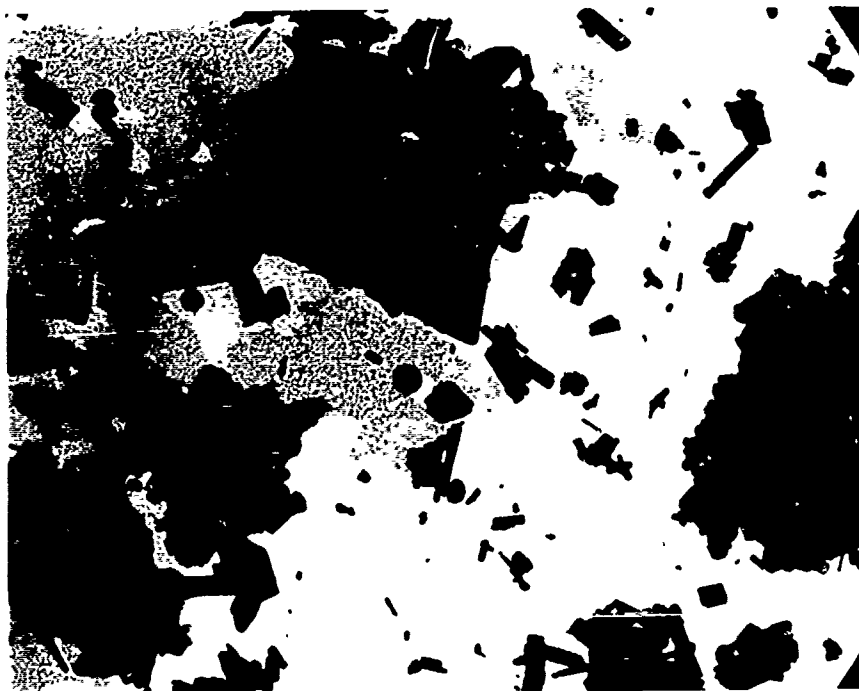


Figure 26. TEM micrograph of the ball milled
St. Joe's #100 ZnO. 12,800X

C. SnO₂

1. Powder Characterization

SnO₂ was the third oxide powder studied. A particle size analysis of the SnO₂, Figure 27, shows a relatively narrow distribution, with approximately 98% of the particles less than 4μm. Also, Figure 28 shows that the particles are reasonably equiaxed. The isoelectric point reported the SnO₂ is between pH 5 and 7.³³

2. Viscosity versus pH

The effect of pH on the viscosity of an 11% solids by volume slip was measured and the results shown in Figure 29. The Brookfield viscometer, using Spindle 4 and a speed of 20 RPM, was used to measure the viscosity. Maximum dispersion occurred at a pH of approximately 11.2. The viscosity steadily increased with decreasing pH, until minimum dispersion occurred at a pH of approximately 3. The viscosity then decreased with lowering pH.

3. Casting

The pH versus centrifugal packing density results are shown in Figure 30. Again, 2.0 grams of powder were dispersed in 14 ml of solution. Centrifuging took place at 6000 RPM for 15 minutes. Higher packing densities occurred at low and high pH values, with lower densities in the middle pH range, which corresponds to the viscosity versus pH data. The highest packing density achieved was 48.0% of the theoretical, which occurred at a pH of 1.

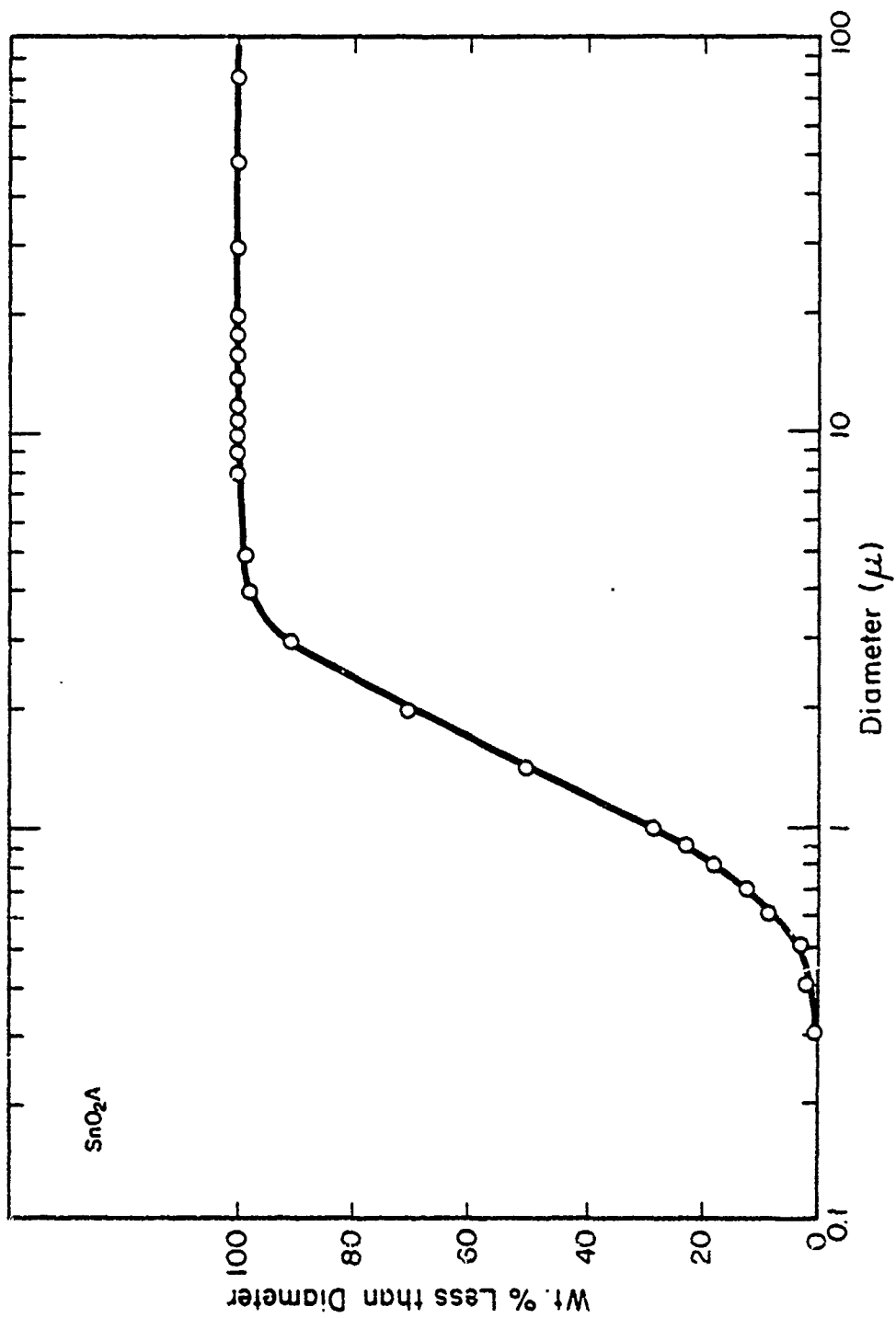


Figure 27. The particle size distribution of the SnO₂.



Figure 28. TEM micrograph of the SnO₂.
12,800X

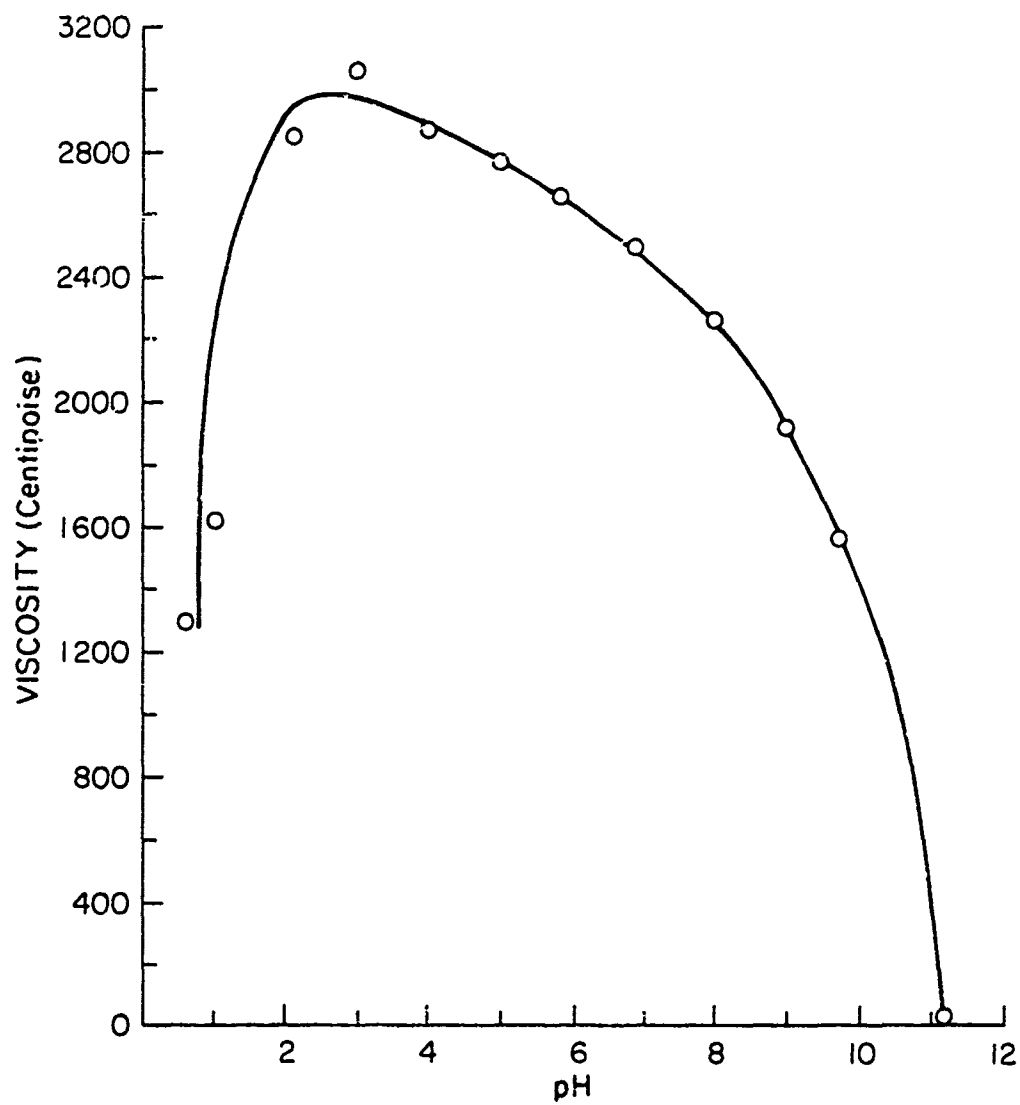


Figure 29. The effect of pH on the viscosity of the slip for the SnO₂.

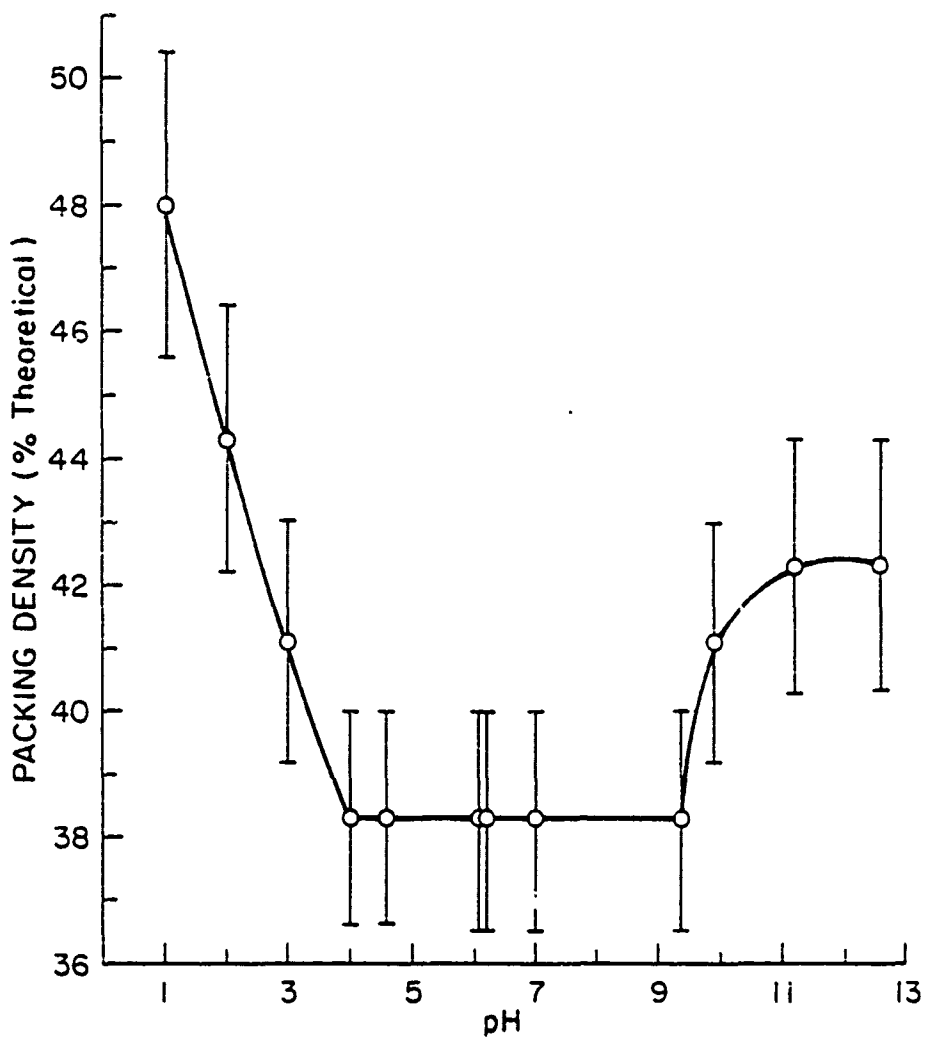


Figure 30. The effect of pH on the centrifugal packing density for the SnO₂.

Two grams of SnO_2 were also dispersed in feeding solution and centrifuged at 7500 RPM for 15 minutes. A 44.3% packing density was obtained. Another 2.0 grams was allowed to settle by gravity in the feeding solution for a few days. All of the powder did not settle in this time period; therefore, it was centrifuged at 7500 RPM for 15 minutes. A 48.0% packing density was achieved. Pellets that were attempted to be fabricated at 11,000 RPM, using a dispersing solution with a pH of 12, cracked during drying.

The particle size distribution of the powder was then lowered by allowing all the particles larger than 2μ to settle out of the suspension. The remaining particle size analysis is shown in Figure 31 which shows that 96% of the particles were less than 2μ .

Two grams of this powder were then dispersed in pH solutions of 12 and 13, and in the feeding solution. These samples were then centrifuged at 7500 RPM for 30 minutes. A 48.0% theoretical packing density was achieved with the pH solution of 12, and a 44.3% packing density was observed in the other two dispersants.

Finally, the results of the centrifugal packing density study as a function of the concentration of powder in the slip (original powder), is and shown in Figure 32. The feeding solution was used as the dispersant in this experiment. The data generally show an increase in packing

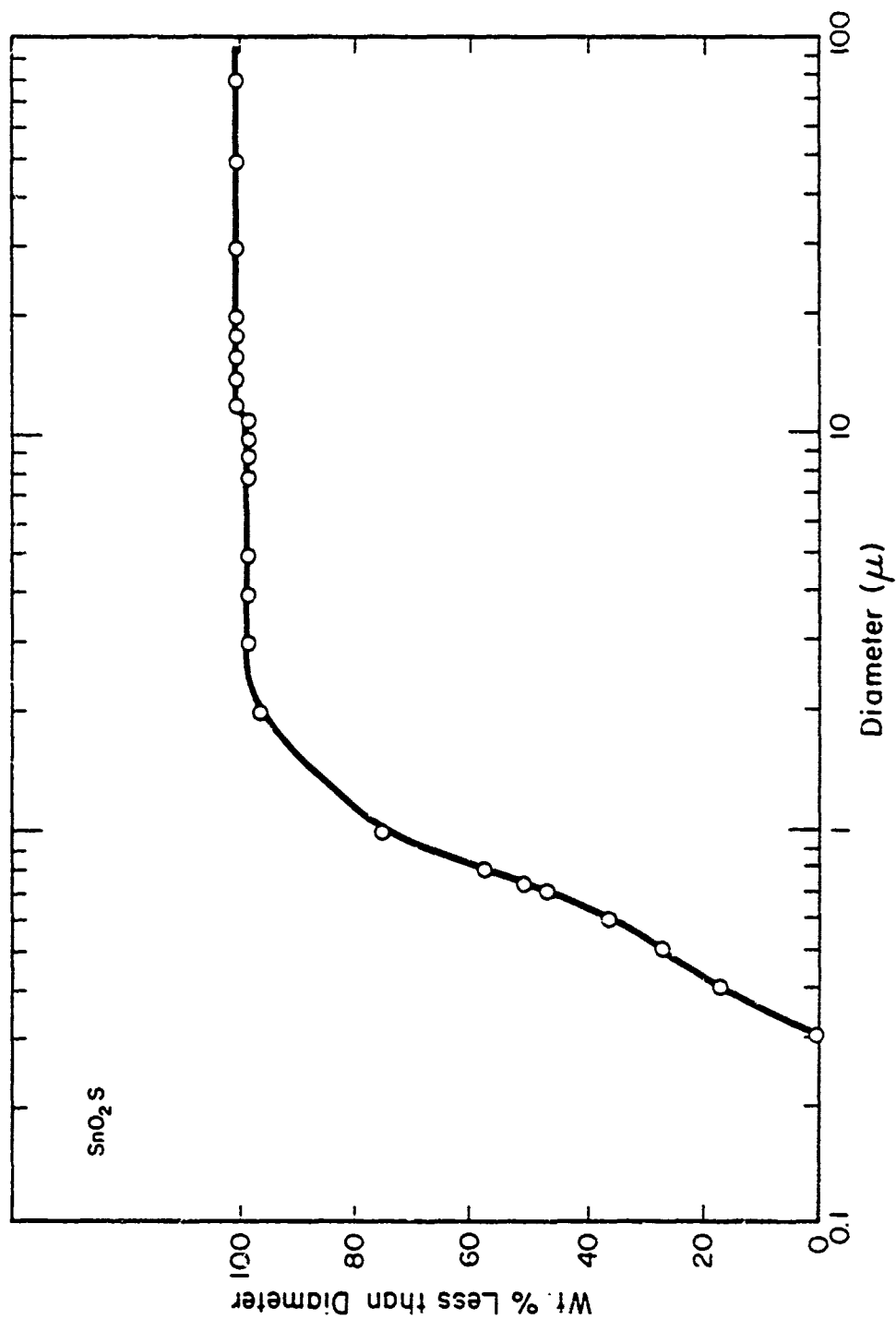


Figure 31. The particle size distribution of the SnO₂ after the larger particles were removed by settling.

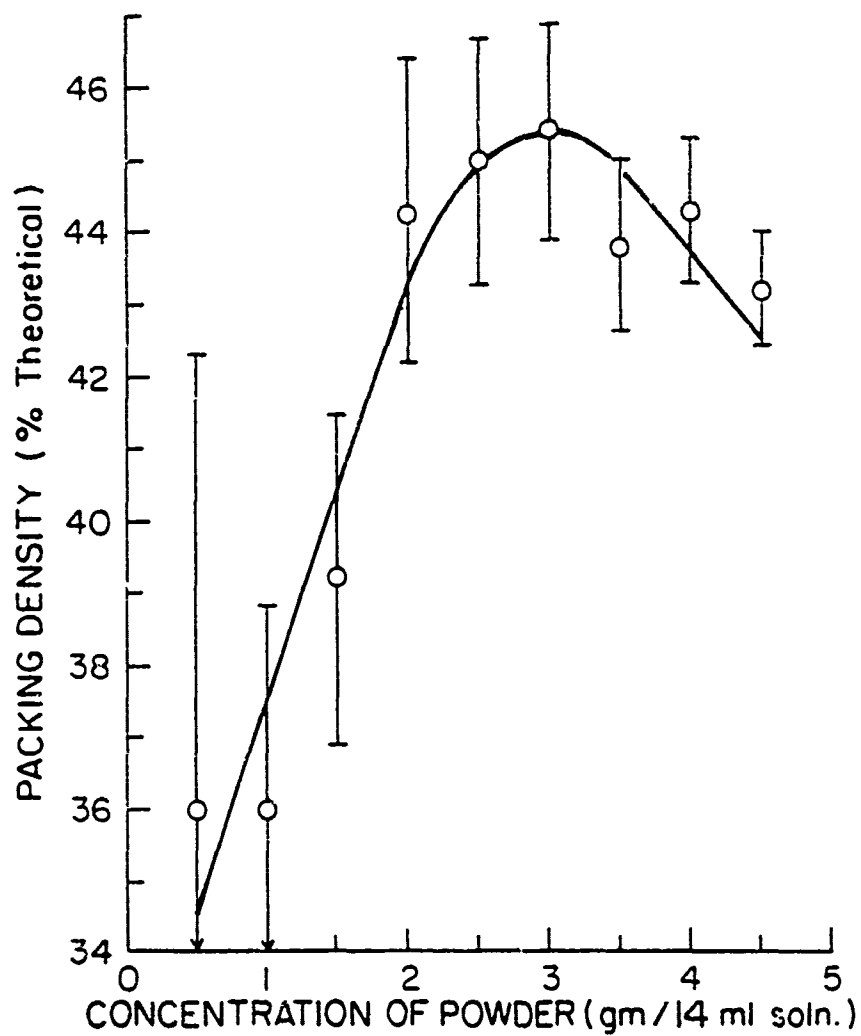


Figure 32. The effect of the concentration of powder in the slip on the centrifugal packing density of the SnO₂.

density as the powder concentration increases. The highest density achieved was 45.4% of the theoretical.

D. Al_2O_3

1. Powder Characterization

Three alumina powders were considered for casting experiments. The first was a 0.1 μm polishing alumina.* The second was Alcoa A-17** used specifically for slip casting and the third was Reynolds RC-152.***

Figure 33 shows the particle size distribution for the 0.1 μm Al_2O_3 . As can be seen, the powder is definitely not 0.1 μm in size. Figure 34 gives the distribution for the Alcoa powder. Here, approximately 99% of the particles are less than 20 μm . Finally, the distribution for the Reynolds powder, Figure 35, shows 98% of the particles less than 8 μm .

SEM micrographs of each of the powders are given in Figures 36-38. Figure 36 shows why the distribution of the polishing alumina is so high. The particle size may be 0.1 μm , however, the powder consists of large agglomerates

* Type B alumina, Fisher Scientific Co., Fairlawn, N.J.

** Alcoa, Chemical Division, Bauxite, Ark.

*** RC-152 DEM (sample 72-8), Reynolds Metal Co., Alumina Research Division, Bauxite, Ark.

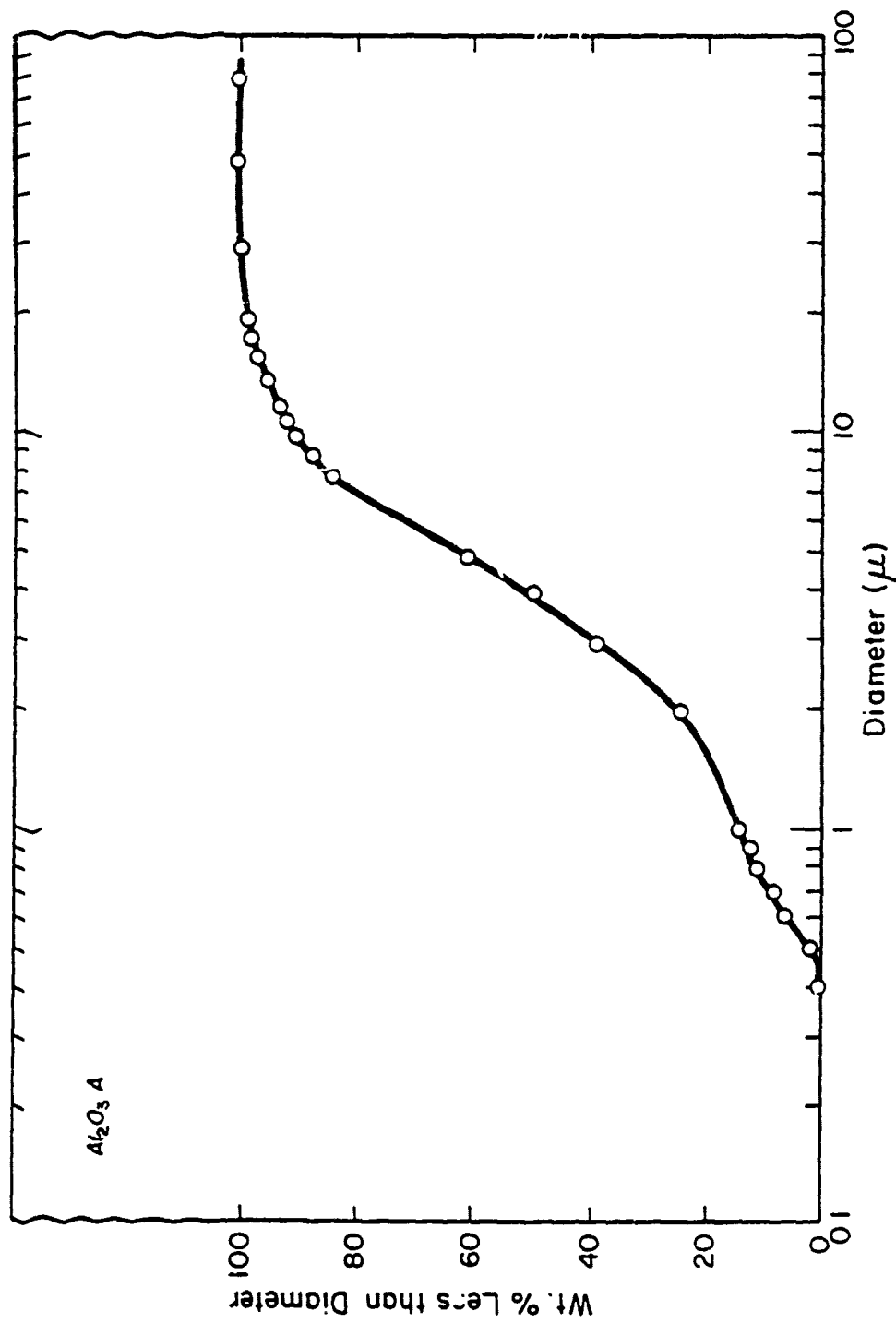


Figure 34. The particle size distribution of the Alcoa A-17 Al₂O₃.

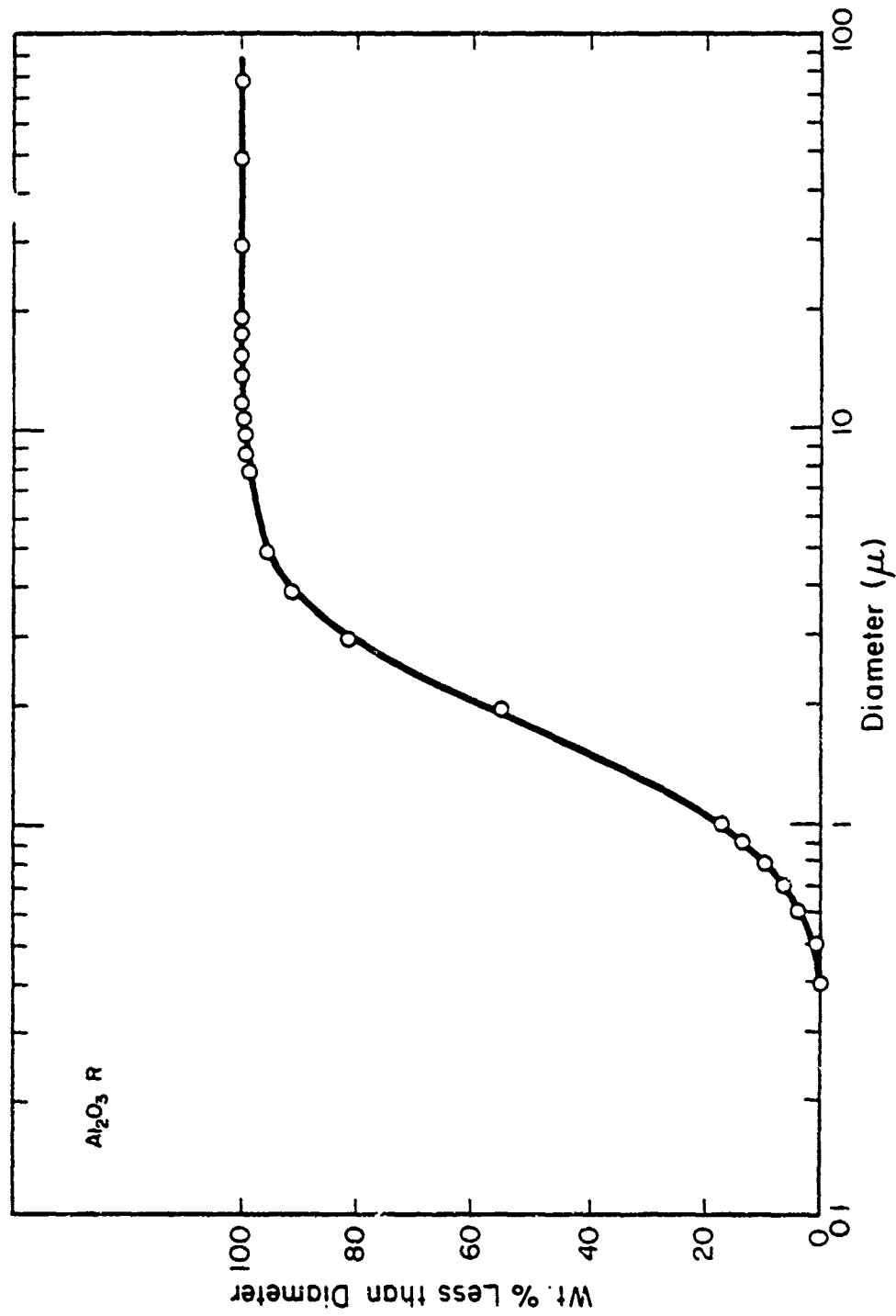


Figure 35. The particle size distribution of the Reynolds RC-152 Al_2O_3 .

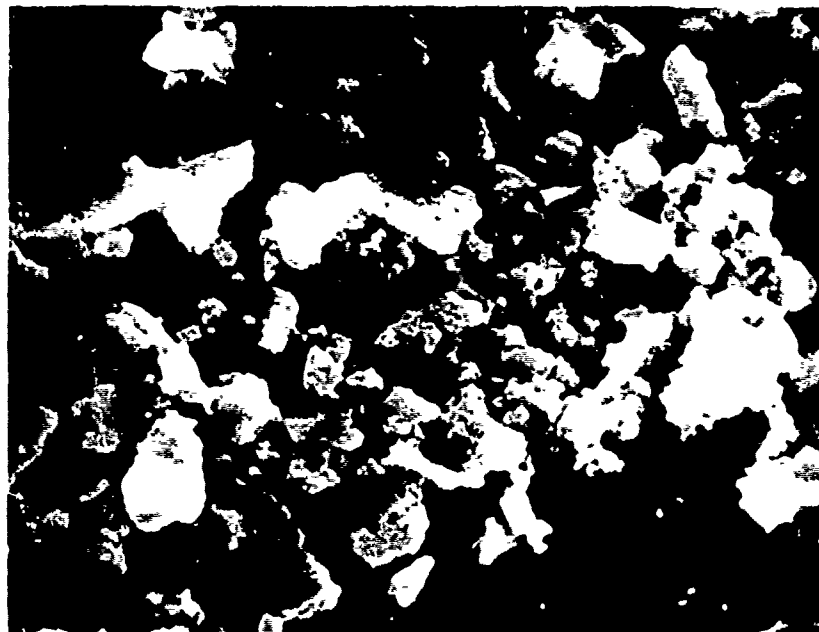


Figure 36. SEM micrograph of the .1 polishing Al_2O_3 from Fisher Scientific Co. 700X



Figure 37. SEM micrograph of the Alcoa A-17 Al_2O_3 . 3000X.

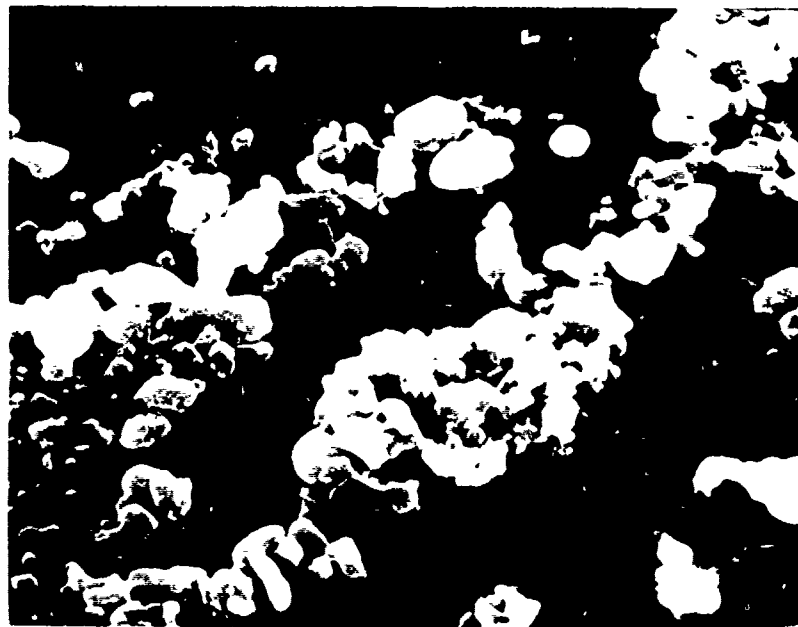


Figure 38. SEM micrograph of the Reynolds RC-152
Al₂O₃. 5000X

of these fine particles. Figure 37 shows the micrograph for the Alcoa alumina. It consists of irregular shaped particles that do not appear to be agglomerated. Finally, Figure 38 shows the Reynolds powder. This powder consists of irregular shaped particles that are more rounded than the Alcoa particles. This powder also appears to be nonagglomerated.

The Reynolds powder appeared to be the most appropriate powder to work with, because of its narrow particle size distribution and acceptable particle shape. However, the Alcoa A-17 alumina was chosen, since it has been proven to give slips with high specific gravities, and slip cast ware with high green densities. The specific gravity of the A-17 was measured to be 3.92. The specific gravity of Al_2O_3 recorded in the literature is 3.97. Since the two values are so close, 3.97 will be used for the calculations recorded in this section.

2. Viscosity versus pH

Viscosity versus pH experiments were then performed on the alumina. Two different slips were prepared. The first had approximately 37% solids by volume and the second had approximately 20% solids by volume. The Brookfield viscometer with spindle 3 and a speed of 20 RPM was used for the 37% solids slip, and a speed of 50 RPM for the 20% solids slip. Two trials were performed on each slip. The

results are shown in Figures 39 and 40. All four curves follow the same trend and agree well with the literature.¹⁹ The isoelectric point of alpha alumina is reported to be between pH 8 and 10.³⁰

3. Casting

Centrifugal packing density studies as a function of pH were the next experiments performed on the alumina. Again, HCl and NH₄OH were the dispersants used, and 20 grams of powder were dispersed in pH solutions of this acid and base. The suspensions were centrifuged until all the powder was packed. The results are shown in Figure 41. Two sets of data were used to prepare one curve, with the difference between the points in each set of data being used as the error limits. The plot shows very peculiar behavior with three maxima and three minima, which appeared in both runs identically, with the highest packing density, 50.4%, occurring at a pH of .8. From the viscosity versus pH data, the lowest viscosity occurred at a pH of 11.

Another sample of the 37% solids slip was prepared. Half of it was adjusted to a pH of 11 and half was adjusted to a pH of 2. Three samples of each of these slips were then centrifugally cast at 6000 RPM for 45 minutes. Part of each slip was also slip cast into a plaster mold. The densities at each pH for each method of formation were determined. The results are tabulated in Tables 5 and 6.

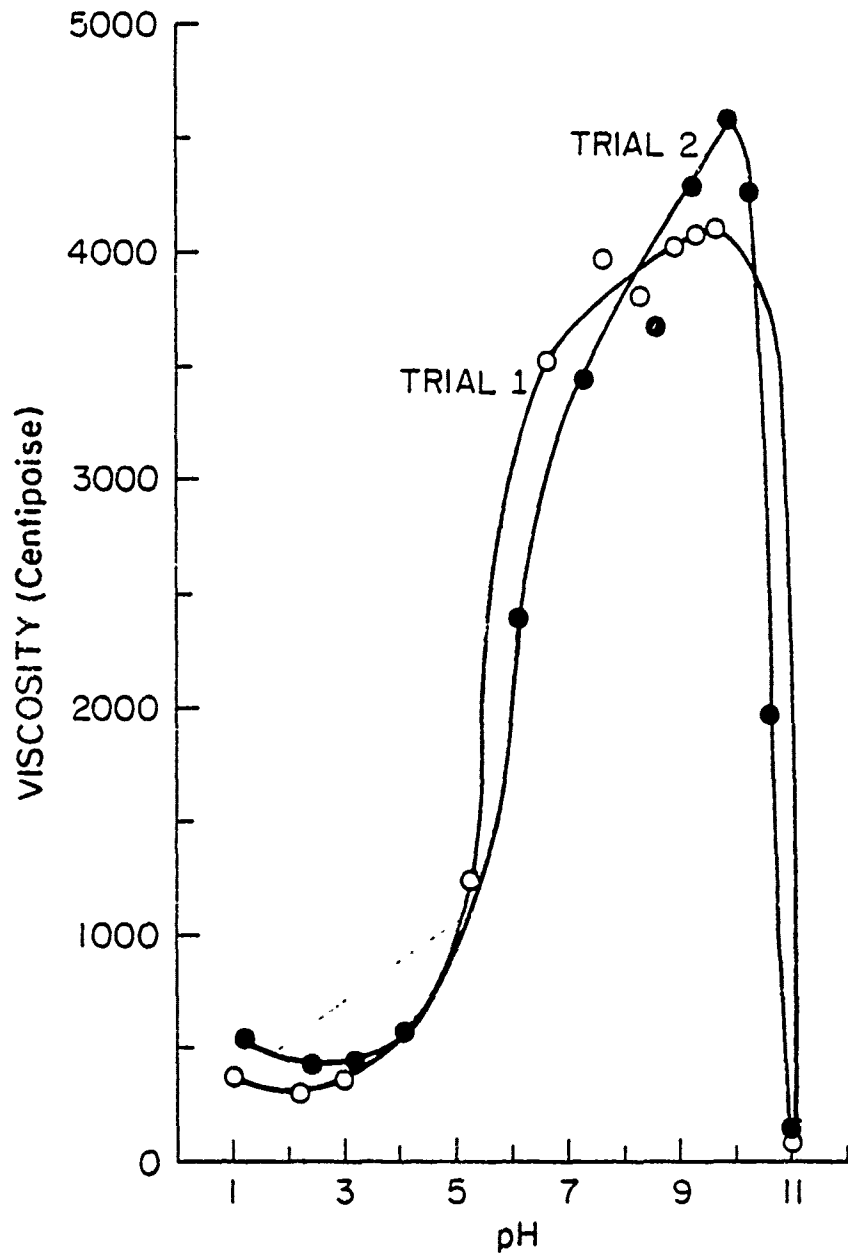


Figure 39. The effect of pH on the viscosity of a 73% solids by volume slip of the Alcoa A-17 Al_2O_3 .

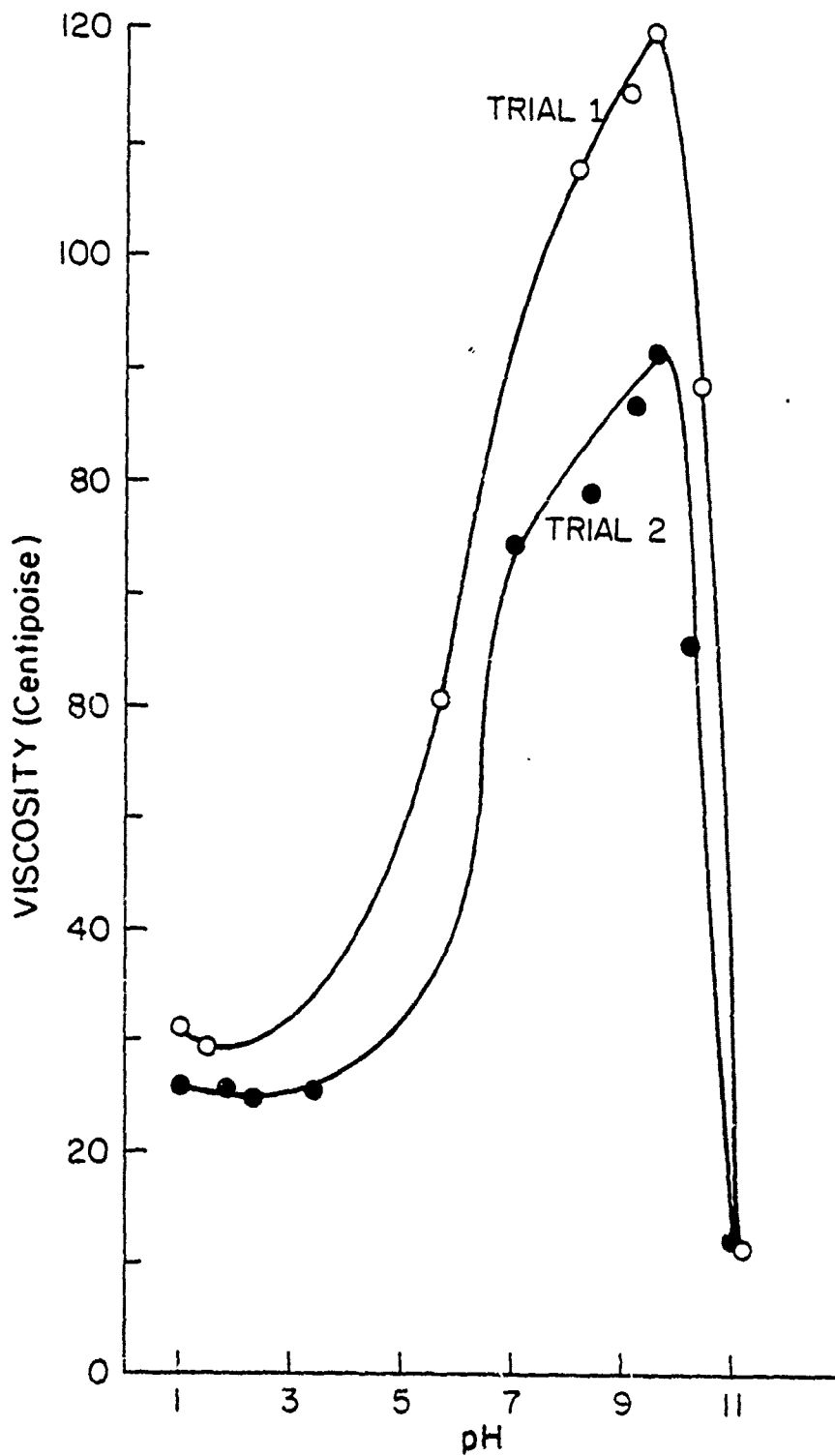


Figure 40. The effect of pH on the viscosity of a 20% solids by volume slip of Alcoa A-17 Al_2O_3 .

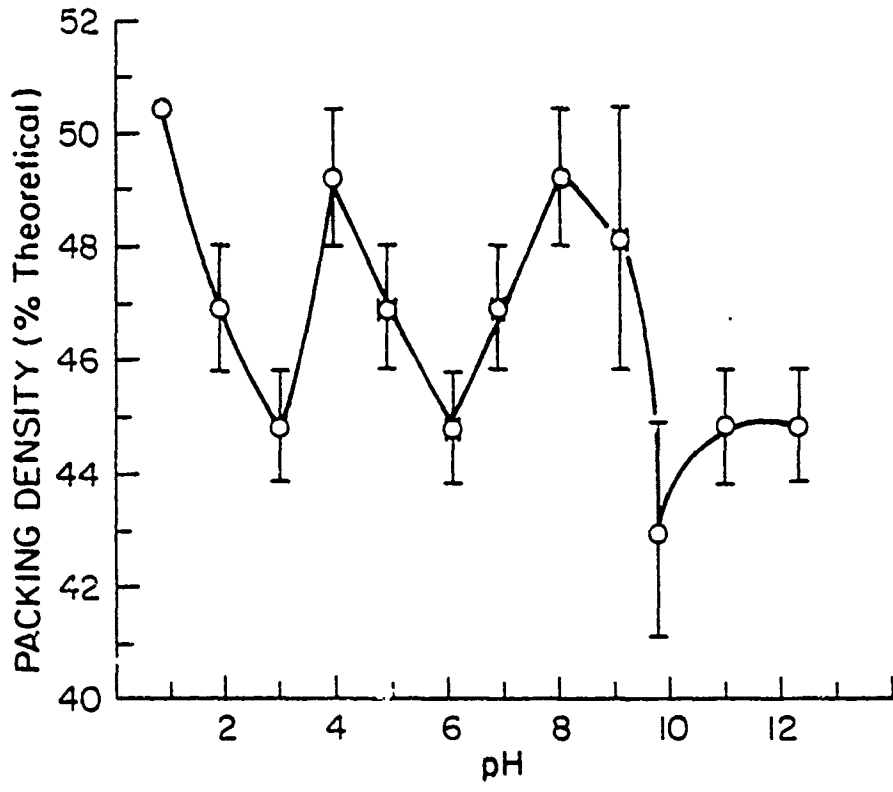


Figure 41. The effect of pH on the centrifugal packing density for the Alca A-17 Al_2O_3 .

Table 5. Centrifugally Cast Packing Densities of 374 solids by Volume Alcoa A-17 Al₂O₃ Slip at pH 2 and 11.

pH	A Wt. of test tube and Powder after Drying (gms)	B Wt. of Empty Test Tube (gms)	A B Weight of Powder (gms)	Packing Volume (cm ³)	Packing Density (% Theor.)
11	31.09	12.32	18.77	8.50	55.6
11	31.41	13.01	18.40	8.60	53.9
11	30.83	12.42	18.41	8.60	53.9
2	30.37	12.84	17.53	7.70	57.3
2	29.90	12.38	17.52	7.80	56.6
2	30.23	12.84	17.39	7.80	56.2

Table 6. Packing Density of Slip Cast Alcoa A-17 Al₂O₃, (pH of Slip was 2).

Sample #	Dry Wt. (gms)	W _D Saturated Wt. (gms)	W _{SS} Saturated Suspended Wt. (gms)	Packing Density (% Theor.)
1	26.46	30.53	19.59	60.9
2	17.28	20.03	12.93	51.3
3	32.95	36.62	23.40	62.8

There are two observations worth noting about this experiment. The first is that the slips of pH 2 gave higher packing densities than those at pH of 1.1, which was not predicted by the viscosity versus pH curves. The second is that slip casting in a mold gave higher packing densities than the centrifugal slip casting.

This Al_2O_3 was also dry pressed at 10,000 psi and 15,000 psi, to compare densities with those of the centrifugally cast and slip cast samples. After pressing, the densities of each sample, three samples for each pressure, were measured. The average density of three samples pressed at 10,000 psi was 64.5% of the theoretical, and the average density for samples pressed at 15,000 psi was 66.1%. The pellets made at 15,000 psi had a higher density than those made at 10,000 psi, which was expected; however, it was not expected to find the dry pressed samples to have higher densities than the slip cast and centrifugally slip cast samples.

Finally, a centrifugal packing density study as a function of the concentration of powder in the slip was performed. The data are plotted in Figure 42. Again, as the concentration of powder increases, the packing density increases. The maximum density achieved was 51.9% of the theoretical at a concentration of .71 gms/ml. The feeding solution was used as the dispersant, and the samples were centrifuged at 6000 RPM for 15 minutes.

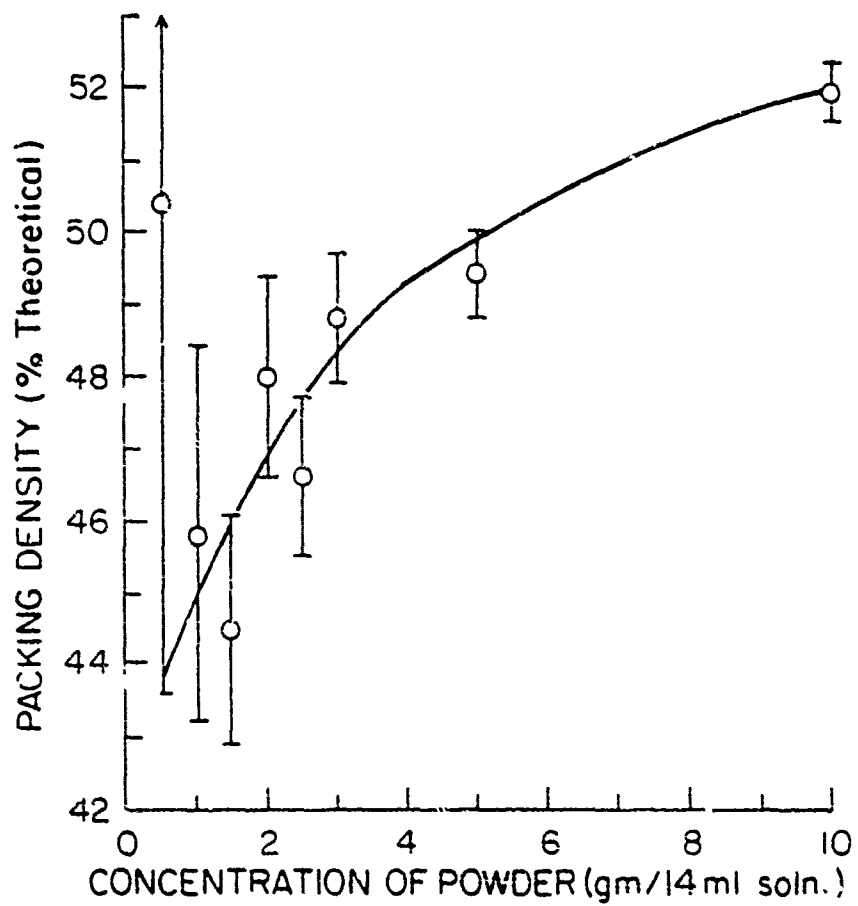


Figure 42. The effect of the concentration of powder in the slip on the centrifugal packing density of the Alcoa A-17 Al_2O_3 .

V. DISCUSSION

A. SiO₂

The 5 μm spherisorb SiO₂ powder was the most ideal for this study because of its narrow particle size distribution and sphericity. The particle size however is perhaps at the large end of the size range in which colloidal behavior is expected. The results of the centrifugal packing density study as a function of pH were disappointing in that high densities were not achieved. The powder that was allowed to settle by gravity attained a slightly higher packing density than that attained by centrifugal casting. This may very well indicate that these particles were too large and that gravity forces dominated their behavior and that they never really formed stable or even semi-stable suspensions.

Increased centrifugal packing densities were obtained with increasing powder content in the slip. This result is predictable and can be explained by:

$$F(x) = \rho g(h-x)$$

where $F(x)$ = the force on the column during centrifuging

at a point x from the bottom;

ρ = the density of the packed column;

$g = (980 \text{ cm/sec}^2) \times (\text{a factor to account for the centrifugal force});$

$h = \text{the height of the packed column.}$

An increase in the amount of powder dispersed in the slip will increase the force on the packed column during centrifuging due to increased h . The density, of course, will vary from the top to the bottom of the packed column, assuming that the density varies with the packing force or pressure. The force at the bottom of a 1 cm. high, 30.4% dense, column of the 5 μm Spherisorb powder that is centrifuged at 6000 RPM would be 62.9 lbs/in².

The centrifugal packing density achieved with the SiO₂ fume was much higher than that achieved with the 5 μm Spherisorb was 30.4% of the theoretical, while the highest density obtained with the SiO₂ fume was 58.1% of the theoretical. The composition of the powders was not the same; however, their densities were comparable. This probably indicates that the smaller silica fume particles were sufficiently small to be dominated by colloidal phenomena rather than gravity. Also, the smaller the particles the longer the settling time for the particles to arrange themselves into closer packing. However, experiments to observe how the settling time affected packing densities of the larger silica particles were not conclusive. In order to increase settling time, the

viscosity of the settling medium was increased. The packing density increased to a maximum and then decreased. It would seem that the density should have continued to increase. This result may be due to the fact that no dispersant was present in the H₂O-glycerine mixtures, and the lack of colloidal behavior.

SEM micrographs, of the packed 5 μ Spherisorb shows that the particles are not arranged in a close packing. However, in areas where the smaller particles, with approximately the same size, are segregated they appear to be uniformly arranged. Larger particles tend to disrupt this arrangement. Therefore, an even narrower particle size distribution may be needed to obtain high packing densities. However, again the probable reason that these powders failed to show the expected improved packing was that their large size allowed gravitational effects to dominate and the classical interplay between surface charge and van der Waals forces never became important.

B. ZnO

The St. Joe #100 that was used for these experiments had a relatively narrow particle size distribution, but the particle shape was undesirable. Nevertheless, the centrifugal slip casting experiments performed on this material produced some interesting results.

The results of the viscosity versus pH experiment were exactly opposite of what was predicted from the solubility and the zpc. The minimum solubility occurs at a pH of approximately 9, which should correspond to the point of minimum dispersion. However, the ZnO had maximum dispersion, minimum viscosity, at this point. The centrifugal packing density as a function of pH results corresponded well with the solubility diagram; however, it was opposite of what was predicted by the viscosity versus pH data. The validity of the viscosity versus pH data is open to serious question due to the fact that the pH changed during the measurement due to the high solubility and apparent rapid dissolution of ZnO at pH values less than nine.

An increase in the centrifugal packing density as the concentration of powder in the slip increased was again observed. This trend appeared with both the original powder and the ball milled powder. This powder also showed a tendency for increased centrifugal packing density with decreased particle size. The increase was from 31.0% of the theoretical density for the original powder to 35.7% for the powder consisting of particles less than 1 μ in size. Finally, an increase in the centrifugal packing density was observed with an improvement in the particle shape. The original powder was ball milled, which destroyed some of the irregular particles and a density of 39.7% of the theoretical was attained.

C. SnO₂

This oxide powder consisted of particles with a narrow particle size distribution and an acceptable shape and size. The viscosity versus pH results show a minimum viscosity at a pH of 11.2. Another minimum occurred at a pH of approximately 0.8. The maximum viscosity occurred at a pH of 3.9 which is consistent with the zpc data.³⁰ The centrifugal packing density as a function of pH showed the trend that was expected from the viscosity versus pH data. A minimum packing density occurred in the middle pH range, with the highest densities being achieved at high and low pH values with the highest density, 48.0% occurring at a pH of one.

As with the other powders, the centrifugal packing density increased with increased powder content in the slip. However, a maximum, appeared to be reached and increasing powder content then tended to lower the packing density. Finally, decreasing the particle size did not increase the packing density for SnO₂.

D. Al₂O₃

Finally, Al₂O₃ was the last oxide that was used for these experiments. The Alcoa A-17 Al₂O₃ did not possess a perfect particle size distribution or particle shape but it has been used specifically for slip casting. This was the major reason it was used for these experiments.

The results of the viscosity versus pH experiments agreed well with the zpc data³⁰ and the literature on slip casting of Al_2O_3 .¹⁹ The viscosity data showed that the maximum dispersion occurred at a pH of 11.

The results of the centrifugal packing density study show reproducibly three minimima and three maximima for reasons which are not completely obvious. Nevertheless, both runs showed exactly the same behavior and therefore it appears to be a real effect. One of the lowest packing densities occurred at a pH of 11 which is opposite to that predicted from the viscosity data. The highest packing density, 50.4% occurred at a pH of one.

Again, the results of the centrifugal packing density as a function of the concentration of powder in the slip showed an increase in density with an increase in the powder content of the slip but not dramatically. The highest packing density achieved was 51.9% of theoretical. Finally, the densities of centrifugally cast, slip cast, and dry pressed samples of the Al_2O_3 were not significantly different.

VI. CONCLUSIONS

The results of the experiments performed in this study indicate some interesting trends. From which the following conclusions have been drawn:

1. Centrifugal slip casting does not appear to enhance the formation of high density castings with typical oxide ceramic powders.
2. Higher centrifugal packing densities are obtained with a decrease in the size of the powder particles.
3. The use of narrower particle size distributions may enhance centrifugal packing densities.
4. An improvement in the particle shape may improve centrifugal packing densities. As shown by the ZnO experiments, a higher packing density was obtained after some of the irregularly shaped particles were reshaped by ball milling.
5. A higher concentration of powder in the slip increases the centrifugal packing density.
6. If there is a relationship between viscosity, taken to be a measure of the degree of dispersion, and packing density, these results did not prove it. Each powder behaved differently but in an individually systematic way.

7. Centrifugal casting does not seem to offer any significant processing advantages over other consolidation techniques for "real world" ceramic powders. Perhaps for more ideal dispersions with unusual precautions it may lead to improved packing density. However, it has yet to be demonstrated.

VII. REFERENCES

1. R.L. Coble and J.E. Burke, "Sintering in Ceramics." p. 197 in *Progress Ceramic Science*, Vol. 3 (Pergamon, Oxford) 1963.
2. T.G. Owe Berg, R.L. McDonald, and R.J. Trainor, Jr., "The Packing of Spheres," *Powder Tech.* 3 183 (1969/70).
3. R.K. McGreary, "Mechanical Packing of Spherical Particles," *J. Amer. Ceram. Soc.*, 44 513 (1961).
4. R.J. Wakeman, "Packing Densities of Particles with Lognormal Size Distribution," *Powder Tech.* II 297 (1975).
5. O.J. Whittemore, Jr., "Particle Compaction," p. 343 in G. Y. Onoda, Jr., and L. L. Hench, eds., *Ceramic Processing Before Firing*, (John Wiley and Sons, N.Y.), 1978.
6. N.G. Stanley-Wood, "The Variation of Pore Sizes in, and the Surface Area of, Powder Compacts of Magnesium Oxide," *Powder Tech.* 12 225 (1975).
7. C. Grescovich and K.W. Lay, "Grain Growth in Very Porous Al_2O_3 Compacts," *J. A. Ceram. Soc.* 55 142 (1972).
8. F.N. Rhines, "Dynamic Particle Stacking," p. 221 in Ref. No. 5.
9. R.L. Coble, "Initial Sintering of Alumina and Hematite," *J. Am. Ceram. Soc.* 41 55 (1958).
10. R.M. German and Z.A. Munir, "Morphology Relations During Surface Transport Controlled Sintering," *Metall. Trans.* 6B 289 (1975).
11. R.M. German and Z.A. Munir, "The Identification of the Initial-Stage Sintering Mechanism: A New Approach," p. 259 in *Sintering and Catalysis*, ref. 10 in *Materials Science Research*, G.C. Kuczynski, ed. (Plenum, N.Y.) 1975.
12. H. Rumpf and H. Schubert, "Adhesion Forces in Agglomeration process," p. 357 of Ref. No. 5.

13. C. Kittel, Introduction to Solid State Physics, 4th ed., (Wiley, N.Y.) p. 102 (1971).
14. E.J.W. Verwey and J.T.G. Overbeek, The Theory of the Stability of Lyophobic Colloids, (Elsevier, N.Y.) 1948.
15. A.R. Cooper, Jr., and L.E. Eaton, "Compaction Behavior of Several Ceramic Powder," J. Am. Ceram. Soc. 45 97 (1962).
16. D.E. Niesz and R.B. Bennett, "Structure and Properties of Agglomerates," p. 61 of Ref. 5.
17. S.J. Lukasiewicz and J.S. Reed, "Character and Compaction Response of Spray-Dried Agglomerates," Bull. Am. Ceram. Soc. 57 798 (1978).
18. J.O'M. Bockrius and A.K.N. Reddy, Modern Electrochemistry, Vol 2, (Plenum, N.Y.) 1970.
19. W.E. Hauth, Jr., "Slip Casting of Aluminum Oxide," J. Am. Ceram. Soc. 32 394 (1949).
20. E.F. Adams, "Slip Cast Ceramics," p. 145 in High Temperature Oxides, 1972.
21. W.H. Rhodes and R.M. Haag, "High Purity Fine Particulate Stabilized Zirconia (Zyttrite)" Rept. No. AFML-TR-70-209, Sept. 1970.
22. Rhodes, W.H., "Agglomerate and Particle Size Effects on Sintering Yttria-Stabilized Zirconia," J. Amer. Ceram. Soc., 64 [1] 19-22 (1981).
23. R.H. Ottewill, "Stability and Instability in Disperse System," J. Colloid and Interface Sci. 58 [2] 357-73 (1977).
24. A. Kose and S. Hachisu, "Ordered Structure in Weakly Flocculated Monodisperse Latex," J. Colloid and Interface Sci. 55 [1] 487-498 (1975).
25. L. Hachisu, et al. "Segregation Phenomena in Monodisperse Colloids," J. Colloid and Interface Sci. 55 [3] 499-509 (1976).
26. J.V. Sanders, "Diffraction of Light by Opals," Acta Cryst. A24 427 (1968).
27. J.V. Sanders, "Microstructure of Silica in Gem Opals" p. 512 in Eighth International Congress on Electron Microscopy, Canberra, Vol. I, 1974.

28. P.J. Darragh, A.J. Gaskin, and J.V. Sanders, Scientific American, 234 84 (1976).
29. Personal Ref., Pieire - Claude Oitcin, Universite de Sherbrooke, Sherbrooke, Que., Canada.
30. G.A. Parks, "The Isoelectric Points of Solid Oxides Solid Hydroxides, and Aqueous Hydroxo Complex Systems," Chem. Revs. [4] 177 (1965).
31. Tapros, Th. F. and Lyklema, J. "Absorption of Potential-Determining Ions at the Silica-Aqueous Electro-Electroanal. Chem., 17 267-275. (1968).
32. Schott, Hans, "Relationship Between Zero Point of Charge and Solubility Product for Hydroxides of Polyvalent Cations," J. of Pharmaceutical Sciences, 66 [11] 1548-1550 (1977).
33. Pourbaix, Marcel, Atlas of Electrochemical Equilibria, (Pergamon Press, New York) 174, 411, 462, (1966).
34. Blok, L. and De Bruyn, P.L. "The Ionic Double Layer at the ZnO/Solution Interface 1. The Experimental Point of Zero Charge," J. of Colloid and Interface Science, 32 [3] 518-526 (1970).

REPORT DISTRIBUTION

A001 - Progress reports as required if letter report. (If technical report, final report distribution is followed followed)

*Scientific Officer - 2/0 ONR Branch
ONR Branch Office - 1/0
ACO - 1/0
Supplemental list if furnished

*Sci.Officer: Dir. Metallurgy & Ceramics Pgm/Dir. Material Sciences Division

A002 - Final Report Distribution

Scientific Officer - 1/0
ONR Branch Office - 1/0
ACO - 1/0
NRL Code 2627 - 6/0* or 1/0**
ONR Code 1021P - 6/0*
DTIC - 12/0* or 2/0**
Supplemental list if furnished

NRL Code 2627 address: (DODAAD Code N00173)
Naval Research Laboratory
Washington, D.C. 20375

DTIC address: (DODAAD Code S47031)
Defense Documentation Center
Bldg. 5, Cameron Station
Alexandria, Virginia 22314

Cognizant ONR Branch Office Address: (DODAAD Code N62880)
536 S. Clark St., Room 286
Chicago, Illinois 60605

Mr. Karsten Styhr/AiResearch Casting Co
19800 Van Ness/Torrance, CA 90509

Paul J. Yancey/Baikowski International Corporation
500 Archdale Drive/Suite 153/Charlotte, NC 28210

*Unclassified/Unlimited report only
**Unclassified/Limited and Classified Reports